



**FACULTY
OF MATHEMATICS
AND PHYSICS**
Charles University

MASTER THESIS

Pavel Press

**One-loop beta-functions of the scalar
couplings in the minimal $SO(10)$ Higgs
model**

Institute of Particle and Nuclear Physics

Supervisor of the bachelor thesis: doc. Ing. Michal Malinský, PhD.

Study programme: Physics

Study branch: Theoretical Physics

Prague 2021

I declare that I carried out this bachelor thesis independently, and only with the cited sources, literature and other professional sources.

I understand that my work relates to the rights and obligations under the Act No. 121/2000 Sb., the Copyright Act, as amended, in particular the fact that the Charles University has the right to conclude a license agreement on the use of this work as a school work pursuant to Section 60 subsection 1 of the Copyright Act.

In date

signature of the author

I would like to thank my supervisor, doc. Ing. Michal Malinský, PhD., for all his help and patience, Mgr. K. Jarkovská for the valuable conversations, and, last but not least, my family and my friends - Lucia and Štěpán - for their support.

Název práce: Jednosmyčkové beta-funkce skalárních vazeb v minimálním $SO(10)$ Higgsově modelu

Autor: Pavel Press

Ústav: Ústav částicové a jaderné fyziky

Vedoucí diplomové práce: doc. Ing. Michal Malinský, PhD., Ústav částicové a jaderné fyziky

Abstrakt: Tato diplomová práce je zaměřena na Minimální $SO(10)$ Teorii velkého sjednocení a konkrétně na její $45 \oplus 126$ Higgsův sektor. Je známo, že ve skalárním spektru tohoto modelu se vyskytují potenciálně tachyonické nestability. Nicméně, tyto problémy mají šanci být vyřešeny pomocí kvantových efektů na úrovni jedné smyčky. To zahrnuje studium druhých derivací efektivního potenciálu. Aby se zajistila stabilita těchto výpočtů, je nutné spočítat beta-funkce skalárních vazeb v Higgsově sektoru. K tomu se váže další aspekt perturbativního přístupu a sice Landauovy póly, které mají tendenci se vyskytovat okolo škály velkého sjednocení. V této práci je spočteno běžení skalárních vazeb ve 45 v $SO(10)$ Higgsově modelu pomocí dvou přístupů: explicitní součet Feynmanových grafů a metoda efektivního potenciálu.

Klíčová slova: Teorie Velkého Sjednocení, rovnice renormalizační grupy, efektivní potenciál

Title: One-loop beta-functions of the scalar couplings in the minimal $SO(10)$ Higgs model

Author: Pavel Press

Institute: Institute of Particle and Nuclear Physics

Supervisor: doc. Ing. Michal Malinský, PhD., Institute of Particle and Nuclear Physics

Abstract: This thesis is focused on the Minimal $SO(10)$ Grand Unified Theory and, in particular, on the $45 \oplus 126$ Higgs sector. It has been shown that in the scalar spectrum of the model there are potentially tachyonic instabilities. However, these issues might be resolved by considering quantum effects at the 1-loop level. This entails the study of the second derivatives of the effective potential. In order to establish the stability of the results of this perturbative approach, it is necessary to evaluate the beta functions of the scalar couplings in the Higgs sector. This way one also addresses the questions regarding the Landau poles of the scalar couplings which tend to be around the unification scale. In this work, the running of the scalar couplings in 45 in the $SO(10)$ Higgs model is evaluated using two approaches: direct summation of Feynman graphs and the effective potential method.

Keywords: Grand Unified Theories, renormalization group equations, effective potential

Contents

Introduction	3
1 Beyond Standard Model	5
1.1 Standard Model and its shortcomings	5
1.2 Grand Unified Theories	7
2 Higgs sector of the $SO(10)$ GUT	10
2.1 Model description	10
2.2 Spontaneous symmetry breaking in $SO(10)$	12
2.2.1 Mass generation	13
2.2.2 Perturbative aspects of the Higgs sector	15
3 Running of the couplings a_0 and a_2 in $SO(4)$ - diagrammatic approach	17
3.1 $SO(4)$ Higgs model	17
3.2 Derivation of the beta functions of a_0 and a_2 within the $SO(4)$ Higgs model	18
3.3 Evaluation of ΔZ_ϕ	21
3.4 Evaluation of K_{a_0} and K_{a_2}	22
3.4.1 Purely scalar contributions to $\Gamma(\phi_{12}\phi_{12} \rightarrow \phi_{12}\phi_{12})$	24
3.4.2 Purely scalar contributions to $\Gamma(\phi_{12}\phi_{13} \rightarrow \phi_{42}\phi_{43})$	29
3.4.3 Contributions to Γ^1 and to Γ^2 proportional to \hat{g}^4	31
3.5 Beta functions of the couplings a_0 and a_2 in $SO(4)$ Higgs model	34
4 Running of the couplings a_0 and a_2 in $SO(10)$ - diagrammatic approach	36
4.1 $SO(10)$ Higgs model description and the beta functions	36
4.2 Evaluation of K_{a_0} and K_{a_2}	37
4.2.1 Purely scalar contributions to $\Gamma(\phi_{12}\phi_{12} \rightarrow \phi_{12}\phi_{12})$	38
4.2.2 Purely scalar contributions to $\Gamma(\phi_{12}\phi_{13} \rightarrow \phi_{42}\phi_{43})$	40
4.2.3 Contributions to Γ^1 and to Γ^2 proportional to \hat{g}^4	42
4.3 Beta functions of the couplings a_0 and a_2 in $SO(10)$ Higgs model	44
5 Effective potential method	46
5.1 Beta functions of the couplings a_0 and a_2 in the $SO(4)$ Higgs model	46
5.2 Beta functions of the couplings a_0 and a_2 in the $SO(10)$ Higgs model	47
Conclusion	49
A Appendix: $SO(10)$ and its representations	51
A.1 Basic definitions	51
A.2 Representations decomposition	52
B Appendix: Integral methods for the DR procedure	55

C Appendix: The interaction term of the $\phi\phi AA$ type	56
D Appendix: Theory of the effective potential method	58
Bibliography	62
List of Figures	65
List of Tables	66
List of Abbreviations	67

Introduction

The search for understanding the fundamental structure of matter has always been one of the core endeavors in physics. In the 20th century, particle physics has enjoyed an immense flourishing thanks to the development of quantum mechanics and quantum field theory, complemented by mathematical advancements in gauge theories. On the experimental side, the arrival of large-scale particle colliders brought forth a bewildering amount of newly discovered particles. All of this led to the formulation of the Standard Model (SM) - a theory describing virtually all of the matter and its interactions we deal with in our every day lives. It is the most successful particle theory there has ever been, as it has been tested to an astounding accuracy and it has stood up to most of the experiments to date. The SM contains 3 generations of fermionic matter consisting of quarks and leptons, 3 fundamental interactions - strong, weak, and electromagnetic force mediated by vector bosons, and last but not least it contains the Higgs field responsible (among other things) for the generation of masses.

Despite all the successes the SM has had over the years it is a known fact that it is *not* the complete theory of matter. This is true even if one ignores the unanswered questions of dark matter, dark energy, and quantum gravity. At the turn of the 21st century, the phenomenon of neutrino oscillations has been conclusively established and this in turn implied that at least 2 neutrinos are massive (albeit very light). This is a clear signal of physics beyond the Standard Model (BSM) since the SM neutrinos are massless. Another phenomenon the SM does not account for is the discrepancy of matter and antimatter we observe in the universe.

There are various directions one can take when addressing the aforementioned issues. One such direction of proposals describing BSM physics present the so-called Grand Unified Theories (GUTs). The core idea of these model is the supposition of new fields residing at large-energy scales which allow for the unification of the three gauge interactions present in the SM. In a sense, it is a relatively straightforward extension of the SM since the structure of a symmetry broken down at low energies is already present in the SM in the electroweak sector. As GUTs contain new fields they also bring new predictions, such as the prediction of the proton decay and magnetic monopoles.

In this thesis, there will be studied the minimal nonsupersymmetric $SO(10)$ GUT, which has been been dismissed in the 1980s as unphysical, because it was thought to suffer from tachyonic instabilities. Recently, this has been shown to be a mere artifact of the tree-level approximation in the perturbation expansion, which has brought back the interest in the theory. In order to tame the tachyonic issues, it is necessary to perform the computations of the 1-loop corrections to the masses in the spectrum of the theory. This also brings up the perturbative aspects of the theory in general, namely the identification of the Landau poles is vital for the analysis of the stability of the predictions with respect to quantum corrections within the theory. In order to understand the structure of higher orders in the perturbative expansion of the theory, it is necessary to evaluate the running of the couplings within the Higgs sector.

The purpose of this thesis is to calculate the beta functions of some of the

scalar couplings in the Higgs sector. In order to understand the quantum corrections better and to have independent checks of correctness, this will be done using two methods: the direct diagrammatic approach and the Coleman-Weinberg effective potential method.

In the first Chapter, a historical and theoretical background of the SM is provided as well as a review of some of its salient features. Some of its shortcomings are explained in more depth and this will motivate its extension in the form of GUTs.

The second Chapter is devoted to a theoretical discussion regarding the Higgs sector in the minimal nonsupersymmetric $SO(10)$ GUT. The model is explicitly defined via the Lagrangian and the Higgs mechanism is described. Subsequently, the tachyonic issues are described in more depth as well as their remedies. Lastly, the study of the perturbative aspects of the theory and, in particular, of the beta functions is provided.

In order to understand the particular structure of the calculations, there is a study of a toy $SO(4)$ Higgs model presented in the third Chapter. The explicit computations are described in detail, as they are much more transparent than in the $SO(10)$ case.

The fourth Chapter is devoted to the calculation of the selected beta functions within the $SO(10)$ GUT, which are the main results of this thesis. Thanks to the work done in the previous chapter, the otherwise complex diagrammatic approach is better understood.

In the fifth Chapter the results from Chapters 3 and 4 are verified. In particular, the beta functions of the selected scalar couplings are evaluated via the effective potential method.

1. Beyond Standard Model

1.1 Standard Model and its shortcomings

Today the most general theory describing the fundamental properties of matter is the *Standard Model of Particle Physics*, which is a self-consistent and renormalizable theory.

The SM is formulated in the language of quantum field theory and it is also a gauge theory with the gauge group being $SU(3) \otimes SU(2) \otimes U(1)$. The corresponding gauge fields mediate the fundamental interactions of matter - $SU(3)$ is responsible for the strong interaction and $SU(2) \otimes U(1)$ is responsible for the weak force and electromagnetism [1], [2]. To this day the SM is being tested and its predictions have been confirmed to an astounding accuracy.

In this context it is perhaps appropriate to bring up the fact that all of the matter which has been directly observed makes up only about 5% of the known universe. The rest is made up of dark matter (about 25%) and dark energy (about 70%). Curiously, the existence of dark matter and dark energy has only been established through the cosmological observation of their effects while their sources remain a mystery.

Putting the questions of dark matter and dark energy aside, it is known that there are other phenomena which the SM does not account for. One such example is the neutrino oscillations, which is the process of neutrinos changing their flavors as they propagate through space and time and it implies that (at least 2) neutrinos are massive. In other words, the neutrinos' flavor and mass eigenstates differ. This effect was conclusively observed at Super-Kamiokande for the case of atmospheric neutrinos [3] and at the Sudbury Neutrino Observatories for the case of solar neutrinos [4].

Another problem unexplained by the SM is the baryon asymmetry problem which refers to the imbalance of baryon matter and antimatter observed in the universe. A simple idea to resolve the question would be to consider the asymmetry as an initial setting of the Big Bang, however, this explanation is widely considered unsatisfactory. A much more natural assumption seems to be that equal amounts of matter and antimatter were created by the Big Bang and thus the overall baryon number would have been equal to zero as an initial setting. If that is the case, there had to exist a process which violated the baryon number and hence created the asymmetry. The SM does in fact allow for a baryon number violation via a non-perturbative processes referred to as sphalerons. In particular, denoting the baryon number density by n_B and the photon density by n_γ , the ratio of baryons to photons given by the theoretical prediction of the SM (via sphalerons) reads

$$\eta_B^{SM} = \frac{n_B}{n_\gamma} \sim \times 10^{-19}. \quad (1.1)$$

However, the result above is in disagreement with the experiments which give the

ratio

$$\eta_B^{exp} = \frac{n_B}{n_\gamma} \sim 6 \times 10^{-10}. \quad (1.2)$$

Therefore, sphalerons cannot explain the observed ratio of matter and antimatter within the SM and so the baryon asymmetry problem remains unresolved.

There are other unresolved issues with the SM, including:

- gravity is not included in the theory
- the hierarchy problem
- the strong CP problem
- the charge quantization

There are many proposals of potential solutions to the mentioned issues but more experimental evidence is needed in order to decide which one is correct.

As was mentioned earlier, there are three fundamental gauge forces described by the SM. The strong nuclear force is mediated by an octet of gluons G_μ^a , which are vector bosons associated to the group $SU(3)$. The group $SU(2) \otimes U(1)$ has four associated gauge bosons where the mass eigenstates are W_μ^+ , W_μ^- , Z_μ , and A_μ . The first three mediate the weak nuclear force while the last one mediates the electromagnetic force.

The fermionic content (also referred to as the matter content) of the SM consists of three generations of quarks and leptons. All these fields interact with each other via the gauge and Higgs fields in an elaborate way. This can be summarized to an extent by their representations shown in the first section of the Table 1.1. The first two numbers in the parenthesis refer to their transformation properties with respect to the groups $SU(3)$ and $SU(2)$, while the last number denotes their *hypercharge*.

Table 1.1: Field content in the SM

Particle type and chirality	Representations
Left-handed Quarks	(3,2,+1/6)
Right-handed up-type Quarks	(3,1,+2/3)
Right-handed down-type Quarks	(3,1,-1/3)
Left-handed Leptons	(1,2,-1/2)
Right-handed Leptons	(1,1,-1)
Higgs (complex scalar)	(1,2,+1/2)
Gluons	(8,1,0)
Weak Gauge Bosons	(1,3,0)
Photon	(1,1,0)

In the second section of the Table 1.1 there is the Higgs scalar doublet. The presence of the doublet is necessary for the Higgs mechanism to take place which spontaneously breaks the symmetry $SU(2)_L \otimes U(1)_Y \rightarrow U(1)_Q$ while generating

masses via Yukawa interactions in a renormalizable way (see [2]). Lastly, the transformation properties of the gauge bosons are given in the last section of the Table 1.1.

1.2 Grand Unified Theories

When one tries to formulate a theory beyond the Standard Model (BSM) it is necessary to make sure the new theory incorporates the SM since so many of its predictions have been confirmed and thus it is clearly a good low-energy effective theory. One class of such BSM theories is called the Grand Unified Theories (GUTs); these offer a natural explanation for the occurrence of neutrino oscillations, baryon asymmetry, and charge quantization.

There exist several hints at the existence of new physics at large energies. One such hint comes from the study of the 1-loop renormalization group equations (RGE) of the running gauge couplings in the SM. The solutions of the equations are known (for a detailed analysis see e.g. [5]). Let the gauge couplings associated with a gauge group be denoted by: g_s for $SU(3)_c$ and g for $SU(2)_L$ and let

$$\alpha_i := \frac{g_i^2}{4\pi}. \quad (1.3)$$

Then the graph of the running gauge couplings takes on a remarkably simple form displayed in Figure 1.1. The fact that the couplings nearly converge suggests that there may be a larger theory unifying the couplings at a scale $M_{\text{GUT}} \sim 10^{16}\text{GeV}$ which is the core feature of GUTs¹. If there were new fields with large masses (so that they would not have been able to be observed by today's colliders), they would affect the running of the couplings and this might then result in exact convergence of the couplings.

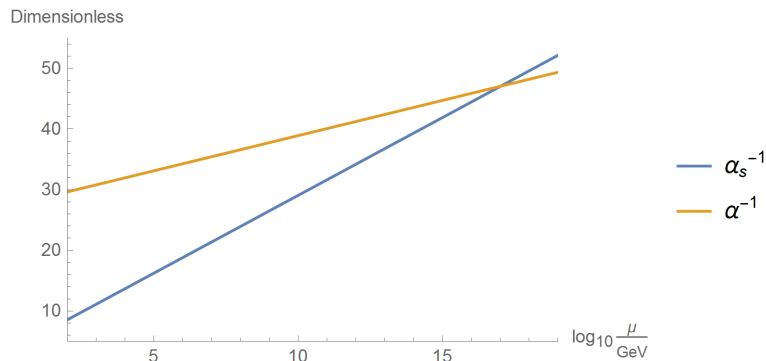


Figure 1.1: Running of the gauge couplings g_s and g in the SM (see [5]).

Another hint of new physics at large energies comes from the seesaw mechanism which is a realistic proposal of a solution of the neutrino oscillations prob-

¹Note that in the Figure 1.1 there is no coupling associated to $U(1)_Y$. The reason for this is that within the SM the overall normalization of the hypercharge is arbitrary. Therefore, the $U(1)_Y$ coupling g' can be rescaled which means it is not relevant for the observations of the large unification scale from the SM point of view. However, once a GUT is constructed the normalization of the hypercharge comes naturally.

lem. The seesaw mechanism can be understood by considering the addition of the non-renormalizable Weinberg d=5 operator to the SM, namely

$$\mathcal{L}_W^{d=5} = \frac{1}{2} c_{\alpha\beta} \left(\overline{L}_\alpha^c \tilde{H}^* \right) \left(\tilde{H}^\dagger L_\beta \right), \quad (1.4)$$

where $L_L = (\nu_L, \ell_L)^T$ is the left-handed lepton doublet of the SM, $\tilde{H} = i\sigma_2 H^*$ with H being the SM Higgs doublet and $c_{\alpha\beta}$ are the elements of a 3×3 complex symmetric matrix. The Weinberg operator generates Majorana mass terms for the neutrinos, in fact, it is the unique operator at d=5 to do so.

In order to formulate a more complete theory, it is necessary to introduce a mediating field which generates $\mathcal{L}_W^{d=5}$ at low energies (this is similar to the case of the Fermi theory and the weak bosons). There are three ways to do that at the tree level, with the mediating fields being a fermionic singlet, a scalar triplet, or a fermionic triplet. The calculation of the masses of the neutrinos and the mediating fields dictate that the mass of the left-handed neutrinos is proportional to the inverse of the mass of the mediating field (the explicit formula depends on the type of the seesaw mechanism). Since the upper bounds for the left-handed neutrinos are very small (eV ballpark), the mass of the mediating fields has to be large and explicit calculations show that it should be close to the M_{GUT} scale (although probably a few orders of magnitude smaller)².

These are some of the main reasons to study GUTs so let's look at how such models come about. First thing one has to think about when formulating a GUT is the gauge group of the theory. It is clear, that all of the content of the SM has to be present within a broader model, which also means that the gauge group of a GUT has to contain the SM gauge group.

Another thing to consider is the fact that in order to have one universal coupling at large energies, the gauge group should be simple. Having these conditions in mind, the candidate with the smallest gauge group is the $SU(5)$ GUT, which was identified by Georgi and Glashow in 1974 [7]. Within the new theory there has to exist a Higgs scalar with a vacuum expectation value (VEV) which spontaneously breaks the $SU(5)$ symmetry into the $SU(3) \otimes SU(2) \otimes U(1)$ symmetry of the SM. This is the same Higgs mechanism, which is present already in the SM and is responsible for the symmetry breaking $SU(2)_L \otimes U(1)_Y \rightarrow U(1)_Q$. Unfortunately, the $SU(5)$ GUT suffers from various problems - for example it is greatly disfavored by its prediction of $\sin^2 \theta_W$ (where θ_W is the *weak-mixing angle*) at low energies where it does not coincide with the experimentally measured value. Therefore, in what follows I will focus on the next smallest possible theory which is the $SO(10)$ GUT.

The $SO(10)$ GUT was formulated by Fritzsche and Minkowski in 1975 [8], [9]. The group $SO(10)$ has rank 5 as opposed to the SM gauge group which has rank 4. This allows for multiple stages in the symmetry breaking process down to the SM gauge group and there also exist various breaking chains with different intermediate stages (for details see [10], [11]).

Since the $SO(10)$ gauge group is 45-dimensional, it contains new gauge bosons mediating new interactions compared to the SM which has a 12-dimensional gauge

²In principle, the mediating field which generates the Weinberg operator does not necessarily have to have a large mass. It could also be that the corresponding Yukawa coupling is very small.

group. This in turn generates new predictions of GUTs, for example the aforementioned proton decay. Particularly, the minimal $SO(10)$ GUT described in [10], [12] is very interesting for the near future experiments, because it has very robust predictions for the proton lifetime which are in the vicinity of today's limits³. In about a decade, the observatory Hyper-Kamiokande [13] should achieve at least an order of magnitude more, which would then tell us more about matter stability. Another striking prediction of GUTs is the existence of magnetic monopoles [14], [15].

³E.g. in Super-Kamiokande the measured lower limit for the proton decay is around 10^{34} yr

2. Higgs sector of the $SO(10)$ GUT

2.1 Model description

A key ingredient to any GUT is a Higgs sector, which is responsible for the spontaneous symmetry breaking while generating masses for the fields in the theory. This thesis is mainly focused on the minimal non-SUSY $SO(10)$ GUT described in detail in [10]. In this model the Higgs fields belong to the direct sum $\mathbf{45} \oplus \mathbf{126}$ of $SO(10)$ where the $\mathbf{45}$ denotes the adjoint representation and $\mathbf{126}$ denotes the self-dual 5-index antisymmetric tensor irreducible representation. In what follows, the real Higgs field in $\mathbf{45}$ will be denoted by ϕ_{ij} and the complex Higgs field in $\mathbf{126}$ by Σ_{ijklm} . The complex conjugated representation will be denoted by Σ_{ijklm}^* . These representations' properties can be also expressed by the equations

$$\begin{aligned}\phi_{ij} &= -\phi_{ji} && \text{(antisymmetry)} \\ \Sigma_{[ijklm]} &= \Sigma_{ijklm} && \text{(antisymmetry)} \\ \Sigma_{ijklm} &= -\frac{i}{5!} \epsilon_{ijklmnopqr} \Sigma_{nopqr} && \text{(self-duality)}\end{aligned}\tag{2.1}$$

where ϵ is the fully antisymmetric Levi-Civita tensor determined by the convention $\epsilon_{12345678910} = +1$ and a sum over repeating indices is implicit (for the rest of the thesis).

The Higgs sector of the $SO(10)$ GUT is defined in the following way [10]. The $SO(10)$ generators $(\hat{T}^{\alpha\beta})_{ij}$ are defined as

$$(\hat{T}^{\alpha\beta})_{ij} = -\frac{i}{\sqrt{2}} (\delta_{\alpha i} \delta_{\beta j} - \delta_{\alpha j} \delta_{\beta i})\tag{2.2}$$

and the gauge fields $A_\mu^{\alpha\beta}$ in the adjoint representation satisfy

$$(A_\mu)_{ij} = \frac{1}{2} A_\mu^{\alpha\beta} (\hat{T}^{\alpha\beta})_{ij}.\tag{2.3}$$

From these building blocks the covariant derivatives are constructed as

$$\begin{aligned}D_\mu \phi_{ij} &= \partial_\mu \phi_{ij} - ig [A_\mu, \phi]_{ij} \\ D_\mu \Sigma_{ijklm} &= \partial_\mu \Sigma_{ijklm} - ig \left\{ (A_\mu)_{ia} \Sigma_{ajklm} + (A_\mu)_{jb} \Sigma_{ibklm} + \right. \\ &\quad \left. + (A_\mu)_{kc} \Sigma_{ijclm} + (A_\mu)_{ld} \Sigma_{ijkdm} + (A_\mu)_{me} \Sigma_{ijkle} \right\}.\end{aligned}\tag{2.4}$$

The gauge field tensor is defined in the standard way by

$$(F^{\mu\nu})_{ij} = \partial^\mu (A^\nu)_{ij} - \partial^\nu (A^\mu)_{ij} - ig [A^\mu, A^\nu]_{ij}\tag{2.5}$$

Finally, the kinetic part of the Higgs model has the following form

$$\mathcal{L}_{kin} = \frac{1}{4} (F_{\mu\nu})_{ij} (F^{\mu\nu})_{ij} + \frac{1}{4} (D_\mu \phi)_{ij}^\dagger (D^\mu \phi)_{ij} + \frac{1}{5!} (D_\mu \Sigma)_{ijklm}^\dagger (D^\mu \Sigma)_{ijklm}. \quad (2.6)$$

The renormalizable potential of the introduced Higgs fields has the general form

$$\begin{aligned} V_0(\phi, \Sigma, \Sigma^*) &= V_\phi(\phi) + V_\Sigma(\Sigma, \Sigma^*) + V_{\text{mix}}(\phi, \Sigma, \Sigma^*) \\ V_\phi(\phi) &= -\frac{\mu^2}{4} (\phi\phi)_0 + \frac{a_0}{4} (\phi\phi)_0 (\phi\phi)_0 + \frac{a_2}{4} (\phi\phi)_2 (\phi\phi)_2, \\ V_\Sigma(\Sigma, \Sigma^*) &= -\frac{\nu^2}{5!} (\Sigma\Sigma^*)_0 + \frac{\lambda_0}{(5!)^2} (\Sigma\Sigma^*)_0 (\Sigma\Sigma^*)_0 + \frac{\lambda_2}{(4!)^2} (\Sigma\Sigma^*)_2 (\Sigma\Sigma^*)_2 + \\ &\quad + \frac{\lambda_4}{(3!)^2 (2!)^2} (\Sigma\Sigma^*)_4 (\Sigma\Sigma^*)_4 + \frac{\lambda'_4}{(3!)^2} (\Sigma\Sigma^*)_{4'} (\Sigma\Sigma^*)_{4'} + \\ &\quad + \frac{\eta_2}{(4!)^2} (\Sigma\Sigma)_2 (\Sigma\Sigma)_2 + \frac{\eta_2^*}{(4!)^2} (\Sigma^*\Sigma^*)_2 (\Sigma^*\Sigma^*)_2, \\ V_{\text{mix}}(\phi, \Sigma, \Sigma^*) &= \frac{i\tau}{4!} (\phi)_2 (\Sigma\Sigma^*)_2 + \frac{\alpha}{2 \cdot 5!} (\phi\phi)_0 (\Sigma\Sigma^*)_0 + \frac{\beta_4}{4 \cdot 3!} (\phi\phi)_4 (\Sigma\Sigma^*)_4 + \\ &\quad + \frac{\beta'_4}{3!} (\phi\phi)_{4'} (\Sigma\Sigma^*)_{4'} + \frac{\gamma_2}{4!} (\phi\phi)_2 (\Sigma\Sigma)_2 + \frac{\gamma_2^*}{4!} (\phi\phi)_2 (\Sigma^*\Sigma^*)_2, \end{aligned} \quad (2.7)$$

where the following notation has been used

$$\begin{aligned} (\phi\phi)_0 &= \phi_{ij} \phi_{ij} \\ (\phi\phi)_2 &= \phi_{ij} \phi_{ik} \equiv (\phi\phi)_{jk} \\ (\Sigma\Sigma^*)_0 &= \Sigma_{ijklm} \Sigma_{ijklm}^* \\ (\Sigma\Sigma^*)_2 &= \Sigma_{ijklm} \Sigma_{ijkln}^* \equiv (\Sigma\Sigma^*)_{mn} \\ (\Sigma\Sigma^*)_4 &= \Sigma_{ijklm} \Sigma_{ijkno}^* \equiv (\Sigma\Sigma^*)_{lmno}, \end{aligned} \quad (2.8)$$

and the full contractions are defined by

$$\begin{aligned} (\Sigma\Sigma^*)_2 (\Sigma\Sigma^*)_2 &= (\Sigma\Sigma^*)_{mn} (\Sigma\Sigma^*)_{mn}, \\ (\Sigma\Sigma^*)_4 (\Sigma\Sigma^*)_4 &= (\Sigma\Sigma^*)_{lmno} (\Sigma\Sigma^*)_{lmno}, \\ (\Sigma\Sigma^*)_{4'} (\Sigma\Sigma^*)_{4'} &= (\Sigma\Sigma^*)_{lmno} (\Sigma\Sigma^*)_{lmno}, \\ (\phi)_2 (\Sigma\Sigma^*)_2 &= \phi_{mn} (\Sigma\Sigma^*)_{mn}, \\ (\phi\phi)_4 (\Sigma\Sigma^*)_4 &= \phi_{lm} \phi_{no} (\Sigma\Sigma^*)_{lmno}, \\ (\phi\phi)_{4'} (\Sigma\Sigma^*)_{4'} &= \phi_{lm} \phi_{no} (\Sigma\Sigma^*)_{lmno}, \\ (\phi\phi)_2 (\Sigma\Sigma)_2 &= (\phi\phi)_{jk} (\Sigma\Sigma)_{jk}. \end{aligned} \quad (2.9)$$

In the potential, there are 3 parameters with the dimension of mass $\{\mu, \nu, \tau\}$, then there are 9 real dimensionless parameters playing the role of quartic scalar couplings $\{a_0, a_2, \lambda_0, \lambda_2, \lambda_4, \lambda'_4, \alpha, \beta_4, \beta'_4\}$, and lastly there are 2 complex dimensionless couplings $\{\eta_2, \gamma_2\}$.

With all the necessary definitions at hand, it is now possible to write down the full Lagrangian of the Higgs model which will be studied in this thesis

$$\mathcal{L} = \mathcal{L}_{kin} - V_0(\phi, \Sigma, \Sigma^*). \quad (2.10)$$

To summarize the field content of the Higgs sector of the $SO(10)$ GUT in [10] - there are 45 vector gauge bosons and the Higgs scalars residing in the $\mathbf{45} \oplus \mathbf{126}$. For the details of the decompositions of the representations, see Appendix A.

2.2 Spontaneous symmetry breaking in $SO(10)$

One of the core ingredients of a realistic $SO(10)$ GUT (or any other BSM theory) is that at low energies the model has to coincide with the SM. In order for that to happen, the large gauge group of the $SO(10)$ theory has to be reduced to the one of the SM $SU(3) \otimes SU(2) \otimes U(1)$. This symmetry breaking is achieved via the so-called Higgs mechanism, which is explained in detail in e.g. [17]. This mechanism is also a part of the SM where gauge group $SU(3)_c \otimes SU(2)_L \otimes U(1)_Y$ is broken down to $SU(3)_c \otimes U(1)_Q$.

In order to break the $SO(10)$ symmetry, scalar fields from the Higgs sector need to receive a VEV. There are 3 SM scalar singlets in the $\mathbf{45} \oplus \mathbf{126}$ representation, namely

$$(1, 1, 1, 0)_\phi \quad (1, 1, 3, 0)_\phi \quad (1, 1, 3, +2)_\Sigma, \quad (2.11)$$

where the multiplets are described in the language of the $SO(10)$ subgroup $SU(3)_C \otimes SU(2)_L \otimes SU(2)_R \otimes U(1)_{B-L}$. The reason one looks for the SM singlets in this context is that VEVs cannot break the SM symmetry group in order to end up with the SM low energy theory. The subscripts ϕ or Σ symbolize the fact that the first two multiplets reside in the $\mathbf{45}$ while the third in $\mathbf{126}$. The VEVs of the multiplets (2.11) are denoted by

$$\begin{aligned} \langle (1, 1, 1, 0)_\phi \rangle &= \sqrt{3}\omega_b \\ \langle (1, 1, 3, 0)_\phi \rangle &= \sqrt{2}\omega_r \\ \langle (1, 1, 3, +2)_\Sigma \rangle &= \sqrt{2}\sigma. \end{aligned} \quad (2.12)$$

The VEVs of the real ϕ -fields are real while the VEV of the complex Σ -fields is in general complex. However, through a redefinition of the overall phase of the Σ -fields the VEV σ can be made real as well.

In the case of the $SO(10)$ GUT in [10] the symmetry breaking may take place in multiple stages. Interestingly enough, there is more than one possible intermediate breaking stage. Following [11] and the notation therein, some of the potentially realistic choices for the intermediate symmetry are

$$\begin{aligned} SO(10) &\rightarrow SU(4)_C \otimes SU(2)_L \otimes U(1)_R \rightarrow SU(3)_c \otimes SU(2)_L \otimes U(1)_Y \\ SO(10) &\rightarrow SU(3)_c \otimes SU(2)_L \otimes SU(2)_R \otimes U(1)_{B-L} \rightarrow SU(3)_c \otimes SU(2)_L \otimes U(1)_Y \\ SO(10) &\rightarrow SU(5) \otimes U(1) \rightarrow SU(3)_c \otimes SU(2)_L \otimes U(1)_Y. \end{aligned} \quad (2.13)$$

Table 2.1: Summary of the breaking patterns depending on the structure of the VEVs [10]. There is the so-called 'flipped' $SU(5) \otimes U(1)$ scenario in the last column denoted by $5'1_{Z'}$ described in [20], [21].

	$\omega_b \neq 0, \omega_r \neq 0$	$\omega_b = 0, \omega_r \neq 0$	$\omega_b \neq 0, \omega_r = 0$	$\omega_b = \omega_r \neq 0$	$\omega_b = -\omega_r \neq 0$
$\sigma = 0$	$3_c 2_L 1_R 1_{B-L}$	$4_c 2_L 1_R$	$3_c 2_L 2_R 1_{B-L}$	$5 1_Z$	$5' 1_{Z'}$
$\sigma \neq 0$	$3_c 2_L 1_Y$	$3_c 2_L 1_Y$	$3_c 2_L 1_Y$	5	$3_c 2_L 1_Y$

A few explanatory remarks are in order here: the subscripts c stand for *color*, L and R stand for *left* and *right*, Y stands for *hypercharge*, and $B - L$ stands for (*baryon number*) - (*lepton number*), where the (*baryon number*) is defined as $1/3$ for quarks and 0 for other fields and the (*lepton number*) is defined as 1 for leptons and 0 for other fields. The symmetry breaking of $SO(10)$ is facilitated by the **45** while the symmetry breaking of the intermediate stage is by the **126**.

Regarding the intermediate stage corresponding to the gauge group $SU(5) \otimes U(1)$, this scenario has been shown to be very problematic in terms of phenomenology. This is due to the fact that it is very difficult to satisfy the current limits on the proton lifetime as well as the SM gauge couplings unification condition, which is a must in a GUT. For this reason, this option is ultimately discarded.

There are several ways how to set up the VEVs which imply various breaking patterns. These breaking patterns are summarized in the Table 2.1. The phenomenologically favored structure of the VEVs is the one where σ corresponds to the seesaw scale. One of the other two VEVs in **45** then corresponds to the larger scale of the grand unification [19].

2.2.1 Mass generation

So far in this chapter there have been discussed the aspects of the Higgs mechanism regarding the symmetry breaking chains. Another inseparable (and vital) feature of the Higgs mechanism is the generation of masses of the physical fields in the theory. The standard description of the Higgs mechanism in the introductory textbooks (cf. [17]) is to take the derivative of the potential with respect to all its variables (i.e. fields) and equate the obtained expressions to 0 . This way one has formulated the conditions for all the stationary points of the potential and now it may be possible to find a minimum having the residual symmetry, which one desires in a given context. However, this method would be extremely inefficient in the present setting.

In the case of the Higgs sector presented in this section, there was already argued that the fields (2.11) should receive the non-zero VEVs based on the symmetry group requirements. This implies the rest of the (many) scalar fields will have their VEVs equal to 0 . Thus, the proper way to calculate the stationarity conditions here is to plug the three VEVs (2.12) into the Higgs potential (2.7) along with the rest of VEVs (which are equal to 0). Subsequently, one takes the derivatives with respect to three singlets (2.12) and set these derivatives

equal to zero. Afterwards, the three equations (corresponding to the stationarity conditions) can be solved for the parameters $\{\mu, \nu, \tau\}$ with the dimension of mass, giving (cf.[10], [22])

$$\begin{aligned}
\mu^2 &= (12a_0 + 2a_2) \omega_b^2 + (8a_0 + 2a_2) \omega_r^2 + 2a_2 \omega_b \omega_r + 4(\alpha + \beta'_4) |\sigma|^2 \\
\nu^2 &= 3(\alpha + 4\beta'_4) \omega_b^2 + 2(\alpha + 3\beta'_4) \omega_r^2 + 12\beta'_4 \omega_b \omega_r + 4\lambda_0 |\sigma|^2 + \\
&\quad + a_2 \frac{\omega_b \omega_r}{|\sigma|^2} (\omega_b + \omega_r) (3\omega_b + 2\omega_r) \\
\tau &= 2\beta'_4 (3\omega_b + 2\omega_r) + a_2 \frac{\omega_b \omega_r}{|\sigma|^2} (\omega_b + \omega_r).
\end{aligned} \tag{2.14}$$

After these results are plugged back into the potential (2.7) the physical spectrum of theory is revealed. In order to obtain the scalar spectrum explicitly, it is necessary to study the second derivatives of the Higgs potential.

However, once the masses are computed, there appear a few *tachyonic instabilities* in the scalar spectrum. In particular, two pseudo-Goldstone boson multiplets¹ have been found to potentially suffer from this problem (cf. [23], [25]) with their tree-level masses being

$$\begin{aligned}
M_S^2(1, 3, 0) &= 2a_2 (\omega_r - \omega_b) (\omega_b + 2\omega_r) \\
M_S^2(8, 1, 0) &= 2a_2 (\omega_b - \omega_r) (\omega_r + 2\omega_b),
\end{aligned} \tag{2.15}$$

where the fields have been described by their transformation properties with respect to the SM gauge group. Their tachyonicity would imply that the stationary points found above do not correspond to physical vacua - this is referred to as the selected vacuum being unstable. What this means is that the parameters appearing in (2.15) have to be constrained into certain domains in order to make sure the vacuum is stable. Namely, the parameters have to satisfy

$$\begin{aligned}
a_2 &> 0 \\
-2 &< \frac{\omega_b}{\omega_r} < -\frac{1}{2}.
\end{aligned} \tag{2.16}$$

Note that it has been shown that for the case $\tau = 0$ the conditions become (cf. [23], [25], [26])

$$\begin{aligned}
a_2 &> 0 \\
-1 &< \frac{\omega_b}{\omega_r} < -\frac{2}{3}.
\end{aligned} \tag{2.17}$$

Comparing the conditions with Table 2.1, one arrives at the fact that the intermediate breaking stage would have to be in the vicinity of $SU(5)' \otimes U(1)_{Z'}$. As was already mentioned above, this scenario is disfavored due to phenomenology. This is true when one talks about the minimalistic setting of theory, which means that there might exist various extension of the model which would allow for this intermediate symmetry group. However, by introducing more free parameters the theory becomes less predictive and loses simplicity and elegance.

¹Note that these pseudo-Goldstone bosons belong to the **45** in the scalar spectrum.

These observations have been made already in the 1980s and, subsequently the minimal $SO(10)$ unification models with the Higgs fields belonging to the adjoint representation were dismissed as unphysical [23], [25], [26]. Therefore, these models fell out of the spotlight for about 30 years until recently when it has been shown that these drawbacks are in fact mere artifacts of the tree-level approximation [27]. In fact, the tachyonic instabilities can be avoided if one goes to higher orders in the perturbative expansion. The formulae for the masses squared (2.15) then receive corrections and, subsequently, the available domains in the parameter space are adjusted, allowing for more realistic symmetry breaking patterns.

2.2.2 Perturbative aspects of the Higgs sector

The observations made in the previous subsections call for a comprehensive study of all of the masses in the scalar spectrum and their 1-loop corrections. This is an ongoing project and this thesis is effort within that direction. The (non)tachyonicity of the physical masses is studied [10] via the second derivatives of the effective potential [28, 29] in a vacuum. However, these corrections depend on the renormalization scale μ . Therefore, it is important to know the dependence on μ of the scalar parameters appearing in the corrections in order to study the reliability of the results.

A dominant role have the scalar couplings a_0 and a_2 among the others, since they appear not only in the 1-loop corrections but, crucially, a_2 appears already at the tree-level, where it multiplies the (potentially) negative expressions in (2.15). This implies the couplings a_0 and a_2 should be under control which can be studied by calculating their beta functions defined by

$$\beta_{a_i} = \mu \frac{\partial a_i}{\partial \mu}. \quad (2.18)$$

This is related to another issue of the so-called Landau poles which are defined as the scale at which the perturbative approach breaks down. Formally, it is the scale where the sub-leading corrections become too large and thus the perturbative expansion loses validity. A notorious example of this phenomenon is the running of the electric charge in quantum electrodynamics (QED), described in e.g. [30]. Denoting the *effective charge* by $e_{eff}(Q^2)$ and the renormalized coupling by $e_R := e_{eff}(m)$ for an arbitrary energy scale m , it can be shown that the sum of all quantum corrections to the photon propagator made out of vacuum polarization loops (depicted in Figure 2.1) yields the following expression

$$e_{eff}^2(Q) = \frac{e_R^2}{1 - \frac{e_R^2}{12\pi^2} \ln \frac{Q^2}{m^2}}. \quad (2.19)$$

It is now easy to see what is meant by the *pole*, as the effective charge in QED $e_{eff}(\Lambda_{Landau}^2) \rightarrow \infty$, where the Landau pole is $\Lambda_{Landau} \approx 10^{286} eV$.

Going back to the $SO(10)$ Higgs sector, the running scalar couplings in (2.7) tend to have the Landau pole close to the unification scale $M_{GUT} \sim 10^{16} GeV$. This is so because below the unification scale there are way less propagating fields

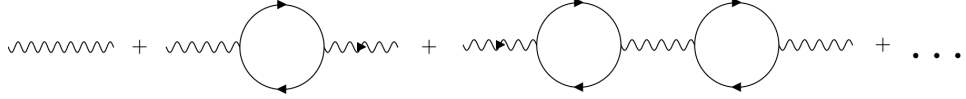


Figure 2.1: The sum of QED vacuum polarization loop corrections to all orders.

than above M_{GUT} (since, e.g., the scalar fields in $\mathbf{45} \oplus \mathbf{126}$ tend to have their masses around M_{GUT}). Therefore, it is natural to expect that the beta functions for the running scalar couplings will have much larger numerical coefficients above the scale M_{GUT} than below it. Thus, the perturbative approach is much more likely to break down above M_{GUT} . In order for the predictions of the theory (e.g. the scalar masses discussed earlier) to be stable with respect to quantum corrections, the running couplings need to be constrained such that their Landau poles appear at higher energies than M_{GUT} .

For the reasons laid out in this section, the Chapters 4 and 5 will be devoted to a detailed computation of the beta functions of the scalar couplings a_0 and a_2 in the Higgs sector of the $SO(10)$ GUT which will be the main results of this thesis. The evaluation of the beta functions of a_0 and a_2 will be done using two methods: the direct diagrammatic approach (Chapter 4) and the Coleman-Weinberg effective potential method (Chapter 5).

Both computational methods will be also presented for an $SO(4)$ toy model in Chapter 3 and in Chapter 5, where the calculations are much simpler. This experience will then prove beneficial for obtaining the main results of this thesis regarding the $SO(10)$ GUT.

It is appropriate to acknowledge that the beta functions of the rest of scalar couplings in the Higgs sector are also necessary for the full analysis of the perturbative aspect of the model. However, that goes beyond the scope of this work.

3. Running of the couplings a_0 and a_2 in $SO(4)$ - diagrammatic approach

For the computation of the desired beta functions of the running couplings in the Higgs sector of $SO(10)$ GUT two methods will be used: the explicit summation of Feynman diagrams and the Coleman-Weinberg effective potential method. The latter of the two is much more convenient and efficient while the former offers perhaps a bit more insight to various contributions and more importantly, it offers an independent check of correctness of the results. It is worth noting that the diagrammatic approach was implemented both by evaluating all of the relevant diagrams by hand and by developing a code in Mathematica, which calculated all of the diagrams. The program confirmed all of the results that will be presented in this chapter.

3.1 $SO(4)$ Higgs model

First, it is appropriate to discuss the reason to study the $SO(4)$ Higgs model. The diagrammatic approach to the evaluation of the beta functions of a_0 and a_2 in the $SO(10)$ Higgs model turns out to be fairly complex. This can be seen by looking at the expression for V_ϕ in the $SO(10)$ Higgs model (2.7) (relevant for the running of the couplings a_0 and a_2) which reads

$$V_\phi = -\frac{\mu^2}{4}(\phi_{ij}\phi_{ij}) + \frac{a_0}{4}(\phi_{ij}\phi_{ij})(\phi_{kl}\phi_{kl}) + \frac{a_2}{4}(\phi_{ij}\phi_{ik})(\phi_{lj}\phi_{lk}). \quad (3.1)$$

In both of the quartic interaction terms in (3.1) there are 4 independent indices running through $\{1, \dots, 10\}$ which amounts to 10^4 individual terms (of course before considering various symmetries of the structure). However, the goal is to calculate the 1-loop beta functions of the couplings a_0 and a_2 within the $SO(10)$ Higgs model. Therefore, the product $\mathcal{L}(x)\mathcal{L}(y)$ needs to be evaluated, which contains 10^8 terms just based off of the number of indices and their domains. The fact that the number of the individual interaction terms is so large makes the explicit evaluation of all relevant Feynman diagrams fairly difficult. For this reason, it appeared to be beneficial to investigate a simpler theory which would still feature the same structure as the $SO(10)$ model.

The aim of this thesis is to compute the beta functions of the scalar couplings a_0 and a_2 in the $SO(10)$ model. Therefore, it will be necessary to evaluate 1-loop contributions to two different 4-point functions of the form $\Gamma(\phi\phi \rightarrow \phi\phi)$ as well as the self-energy diagram for one of the scalar fields (this will be made explicit in sec.4.3). The most convenient choice of the 4-point functions will be shown to be

- $\Gamma^1 = \Gamma(\phi_{12}\phi_{12} \rightarrow \phi_{12}\phi_{12})$
- $\Gamma^2 = \Gamma(\phi_{12}\phi_{13} \rightarrow \phi_{42}\phi_{43})$

In order to simplify the evaluation of Γ^1 and Γ^2 it would be convenient to find the smallest $SO(N)$ Higgs model with the same structure as in (3.1) which would be able to produce such 4-point functions. It is now easy to see that the optimal choice is the $SO(4)$ Higgs model.

For the reasons laid out above, this Chapter will be devoted to the evaluation of the beta functions of the scalar couplings a_0 and a_2 within the $SO(4)$ Higgs model. The Lagrangian of the $SO(4)$ theory has the form

$$\mathcal{L} = \mathcal{L}_{kin} - V_\phi(\phi), \quad (3.2)$$

where

$$\begin{aligned} \mathcal{L}_{kin} &= \frac{1}{4} (F_{\mu\nu})_{ij} (F^{\mu\nu})_{ij} + \frac{1}{4} (D_\mu \phi)_{ij}^\dagger (D^\mu \phi)_{ij} \\ V_\phi &= -\frac{\mu^2}{4} (\phi_{ij} \phi_{ij}) + \frac{a_0}{4} (\phi_{ij} \phi_{ij}) (\phi_{kl} \phi_{kl}) + \frac{a_2}{4} (\phi_{ij} \phi_{ik}) (\phi_{lj} \phi_{lk}). \end{aligned} \quad (3.3)$$

In the expressions above all of the indices now run through $\{1, \dots, 4\}$. The covariant derivatives in (3.3) are defined by the formula (2.4) with the indices again running through $\{1, \dots, 4\}$.

By comparing (3.3) with (2.6) and (2.7) one can infer that the index structure of the $SO(4)$ model is the same as in the $SO(10)$ model. However, since the number of individual interaction terms in (3.2) is much smaller than in the $SO(10)$ scenario (i.e. in (2.6) and (2.7)), the calculations here become much more transparent. This way a lot will be learned from evaluating the beta functions of the scalar couplings a_0 and a_2 within the $SO(4)$ Higgs model. The gained knowledge will then be translated into the calculations within the $SO(10)$ model presented in the next Chapter.

Needless to say, the $SO(4)$ model does not resemble a realistic physical theory of our universe in any shape or form. Its purpose is to merely help understand the structure of the Feynman diagrams.

3.2 Derivation of the beta functions of a_0 and a_2 within the $SO(4)$ Higgs model

The running of the couplings a_0 and a_2 will be calculated in the minimal subtraction (MS) scheme. To begin with, the bare Lagrangian of the theory has the form (following the notation in [32])

$$\begin{aligned} \mathcal{L}_\phi^B &= \frac{1}{4} (D_\mu \phi^B)_{ij}^\dagger (D^\mu \phi^B)_{ij} - \frac{\mu^2}{4} (\phi^B \phi^B)_0 \\ &\quad - \frac{a_0^B}{4} (\phi^B \phi^B)_0 (\phi^B \phi^B)_0 - \frac{a_2^B}{4} (\phi^B \phi^B)_2 (\phi^B \phi^B)_2, \end{aligned} \quad (3.4)$$

where the following notation was used

$$\begin{aligned} (\phi\phi)_0 &= (\phi_{ij} \phi_{ij}) \\ (\phi\phi)_2 (\phi\phi)_2 &= (\phi_{ij} \phi_{ik}) (\phi_{lj} \phi_{lk}). \end{aligned} \quad (3.5)$$

The wave-function renormalization factor Z_ϕ is defined by

$$\phi_{ij}^B = \sqrt{Z_\phi} \phi_{ij} \quad (3.6)$$

where (ij) is an arbitrary pair of indices. It is convenient to recast the factor Z_ϕ as

$$Z_\phi = 1 + \Delta Z_\phi. \quad (3.7)$$

The bare Lagrangian may be expressed in the form

$$\mathcal{L}_\phi^B = \mathcal{L}_\phi + \delta\mathcal{L}_\phi \quad (3.8)$$

where (neglecting the term quadratic in ϕ)

$$\mathcal{L}_\phi = \frac{1}{4} (D_\mu \phi)_{ij}^\dagger (D^\mu \phi)_{ij} - \frac{a_0}{4} (\phi\phi)_0 (\phi\phi)_0 - \frac{a_2}{4} (\phi\phi)_2 (\phi\phi)_2. \quad (3.9)$$

The counterterm-Lagrangian then reads

$$\delta\mathcal{L}_\phi = \Delta Z_\phi \frac{1}{4} (D_\mu \phi)_{ij}^\dagger (D^\mu \phi)_{ij} - \frac{\delta a_0}{4} (\phi\phi)_0 (\phi\phi)_0 - \frac{\delta a_2}{4} (\phi\phi)_2 (\phi\phi)_2. \quad (3.10)$$

The counterterms δ_{a_0} and δ_{a_2} are related to the bare quantities by

$$a_i + \delta_{a_i} = a_i^B Z_\phi^2. \quad (3.11)$$

It is useful to recast the counterterms as

$$\delta_{a_i} = a_i K_{a_i}. \quad (3.12)$$

With the counterterms at hand the bare coupling can be written down as

$$a_i^B = a_i (1 + K_{a_i}) Z_\phi^{-2}. \quad (3.13)$$

The dimensional regularization (DR) procedure with the convention $d = 4 - 2\epsilon$ will be used in what follows. A regularization scale μ with the dimension of mass is introduced into the Lagrangian through the definitions

$$\begin{aligned} \hat{a}_0 &= a_0 \mu^{-2\epsilon} \\ \hat{a}_2 &= a_2 \mu^{-2\epsilon} \\ \hat{g} &= g \mu^{-\epsilon}. \end{aligned} \quad (3.14)$$

With definitions above in mind, the Lagrangian (3.8) within the DR scheme reads

$$\begin{aligned}\mathcal{L}_\phi^{DR} &= \frac{1}{4} Z_\phi (D_\mu \phi)_{ij}^\dagger (D^\mu \phi)_{ij} \\ &\quad - \frac{\hat{a}_0 \mu^{2\epsilon}}{4} (\phi\phi)_0 (\phi\phi)_0 - \frac{\hat{a}_2 \mu^{2\epsilon}}{4} (\phi\phi)_2 (\phi\phi)_2 \\ &\quad - \frac{\hat{a}_0 \mu^{2\epsilon} K_{a_0}}{4} (\phi\phi)_0 (\phi\phi)_0 - \frac{\hat{a}_2 \mu^{2\epsilon} K_{a_2}}{4} (\phi\phi)_2 (\phi\phi)_2.\end{aligned}\tag{3.15}$$

The running of the scalar couplings a_0 and a_2 is given by their corresponding beta functions defined by

$$\beta_{\hat{a}_i} = \mu \frac{\partial \hat{a}_i}{\partial \mu}.\tag{3.16}$$

Plugging the relation (3.14) into (3.16) gives

$$\mu \frac{\partial \hat{a}_i}{\partial \mu} = \mu^{-2\epsilon+1} \frac{\partial a_i}{\partial \mu} - 2\epsilon \hat{a}_i.\tag{3.17}$$

Now, recalling the relation $a_i^B = a_i (1 + K_{a_i}) Z_\phi^{-2}$ and differentiating both sides with respect to μ gives to the leading order

$$\begin{aligned}0 &= \frac{\partial a_i^B}{\partial \mu} = \frac{\partial}{\partial \mu} \left(a_i (1 + K_{a_i}) Z_\phi^{-2} \right) = \\ &= \frac{\partial a_i}{\partial \mu} (1 + K_{a_i} - 2\Delta Z_\phi) + a_i \left(\frac{\partial K_{a_i}}{\partial \mu} - 2 \frac{\partial \Delta Z_\phi}{\partial \mu} \right),\end{aligned}\tag{3.18}$$

where the fact that a_i^B is constant with respect to μ was utilized. Given that the last expression is equal to 0, it can be further recast (to the leading order in powers of the coupling) as

$$\frac{\partial a_i}{\partial \mu} = a_i \left(-\frac{\partial K_{a_i}}{\partial \mu} + 2 \frac{\partial \Delta Z_\phi}{\partial \mu} \right).\tag{3.19}$$

Plugging the last equation into (3.17) gives (neglecting terms $\sim O(\epsilon)$)

$$\beta_{\hat{a}_i} = \mu \frac{\partial \hat{a}_i}{\partial \mu} = \mu^{-2\epsilon+1} a_i \left(-\frac{\partial K_{a_i}}{\partial \mu} + 2 \frac{\partial \Delta Z_\phi}{\partial \mu} \right).\tag{3.20}$$

The eq. (3.20) is the main result of this section as it gives an explicit prescription of the running of the couplings a_0 and a_2 within the $SO(4)$ Higgs model.

The next step is to calculate the quantities K_{a_i} and ΔZ_ϕ which will be described in detail in the following sections.

3.3 Evaluation of ΔZ_ϕ

Within the MS scheme the wave-function renormalization factor $Z_\phi = 1 + \Delta Z_\phi$ is fixed via (see e.g. [30])

$$Z_\phi = 1 + \left. \frac{\partial \Sigma_\phi^{MS}(p^2)}{\partial p^2} \right|_{p^2=m_\phi^2}. \quad (3.21)$$

The quantity $\Sigma_\phi^{MS}(p^2)$ corresponds to the 1-loop corrections to the scalar propagator.

The 1-loop contributions to the scalar propagator relevant for the evaluation of ΔZ_ϕ in (3.21) originate in the term containing covariant derivatives in (3.15). The relevant interaction terms of the form $A\phi\phi$ may be recast as

$$i\hat{g}A_\mu^a \left(\partial^\mu \phi_i^\dagger (T^a \phi)_i - (T^a \phi)_i^\dagger \partial^\mu \phi_i \right). \quad (3.22)$$

Now, it is necessary to evaluate the 1-loop contribution produced by the interaction term (3.22). The Feynman rule corresponding to the vertex produced by this term is given in Figure 3.1. The 1-loop contribution to the scalar propagator coming from (3.22) is shown in Figure 3.2.

Before one can evaluate the integral corresponding to the diagram in Figure 3.2 it is appropriate to discuss the gauge of the vector boson propagator¹. The general form of the propagator in the R_ξ -gauge reads

$$D_\xi^{\mu\nu} = i \frac{-g^{\mu\nu} + (1 - \xi) \frac{l^\mu l^\nu}{l^2 - \xi M^2}}{l^2 - M^2 + i\epsilon}. \quad (3.23)$$

Ultimately, the choice of a particular gauge is a matter of preference as the final beta functions do not depend on it. Throughout this thesis, the *Lorentz gauge* (also referred to as the *Landau gauge*) will be utilized, i.e. $\xi = 0$. This gauge choice has the following advantages:

- The Goldstone bosons have the same scalar couplings as they would in the ungauged scalar model. This means that one has to work with the Lagrangian given in (3.15) and account for the contributions of all the scalar fields therein the same way. This is a welcome feature because one does not need to worry about which degrees of freedom are physical and which are not when it comes to the calculations in this chapter.
- The interaction terms containing the Higgs scalars and the *Faddeev-Popov* ghosts are proportional to ξ . Therefore, thanks to the Lorentz gauge $\xi = 0$ there will be no diagrams with ghosts relevant in this thesis.

The contribution of the self-energy diagram depicted in Figure 3.2 reads (for $\xi = 0$)

$$\Sigma_\phi^{MS}(p^2) = (i)^2 (-1) T_{ij}^a T_{ji}^b \delta_{ab} \hat{g}^2 \mu^{2\epsilon} \int \frac{d^d l}{(2\pi)^d} \frac{i(2p+l)_\mu (2p+l)_\nu}{l^2 - m_\phi^2} D^{\mu\nu}(l). \quad (3.24)$$

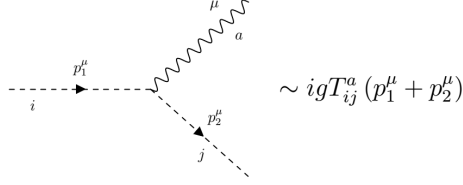


Figure 3.1: Feynman rule corresponding to the interaction in (3.22).

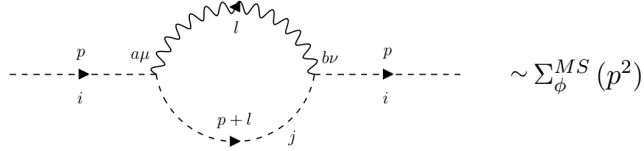


Figure 3.2: The self-energy diagram of a scalar field.

After performing the usual steps - Feynman parametrization and the DR master formula (see Appendix B) - the result is

$$\Sigma_\phi^{MS}(p^2) = \hat{g}^2 C_2(\text{Adj.}) \frac{3}{16\pi^2 \epsilon} p^2 + (\text{irrelevant terms}), \quad (3.25)$$

where $C_2(\text{Adj.})$ is the quadratic Casimir of the adjoint representation. The summand called (irrelevant terms) represents the terms, which vanish or at least are finite after being plugged into (3.21) and therefore those terms will be discarded in what follows ².

The result (3.25) can now be plugged into (3.21) which together with (3.7) yields

$$\Delta Z_\phi = \hat{g}^2 C_2(\text{Adj.}) \frac{3}{16\pi^2 \epsilon}. \quad (3.26)$$

3.4 Evaluation of K_{a_0} and K_{a_2}

The counterterms K_{a_0} and K_{a_2} appear in the Lagrangian in (3.15) as factors of quartic scalar couplings. The corresponding tree diagrams are depicted in Figure 3.3.

In order to fix the counterterms K_{a_0} and K_{a_2} it is necessary to consider two different 4-point functions $\Gamma^1 = \Gamma(\phi_1 \phi_2 \rightarrow \phi_3 \phi_4)$ and $\Gamma^2 = \Gamma(\tilde{\phi}_1 \tilde{\phi}_2 \rightarrow \tilde{\phi}_3 \tilde{\phi}_4)$. The contributions of the counterterms corresponding to the two 4-point functions will be denoted by $\Gamma_{Ka_0}^i$ and $\Gamma_{Ka_2}^i$. Next, the 1-loop contributions to the 4-point functions with the same outer legs $\Gamma_{1loop}^1 = \Gamma(\phi_1 \phi_2 \rightarrow \phi_3 \phi_4)$ and $\Gamma_{1loop}^2 = \Gamma(\tilde{\phi}_1 \tilde{\phi}_2 \rightarrow \tilde{\phi}_3 \tilde{\phi}_4)$ will have to be evaluated. Once these quantities are computed the counterterms will be fixed via the equations (in the MS scheme)

$$\begin{aligned} \Gamma_{1loop}^1 + \Gamma_{Ka_0}^1 + \Gamma_{Ka_2}^1 &\stackrel{!}{=} \text{finite} \\ \Gamma_{1loop}^2 + \Gamma_{Ka_0}^2 + \Gamma_{Ka_2}^2 &\stackrel{!}{=} \text{finite}. \end{aligned} \quad (3.27)$$

¹The discussion of the gauge choice follows [33]

²Note that the calculations in this thesis are done within the MS scheme

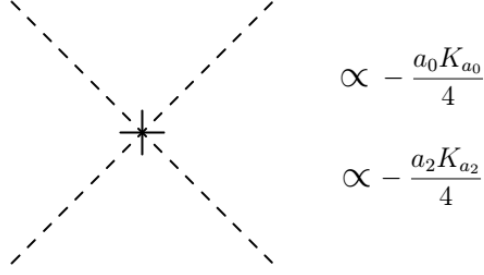


Figure 3.3: Diagram corresponding to the counterterms K_{a_0} and K_{a_2}

The equality ' $\stackrel{!}{=}$ finite' represents the fact that the counterterms K_{a_0} and K_{a_2} absorb only the pole terms, i.e. the terms proportional to $1/\epsilon$.

The outer legs for the 4-point functions Γ^1 and Γ^2 have to be chosen in such a way that the two equations in (3.27) are linearly independent. In order to identify which 4-points functions can be calculated it is convenient to expand the quartic scalar interaction terms in (3.15).

The \hat{a}_0 -term in (3.15) gives

$$\begin{aligned}
\mathcal{L}_{\hat{a}_0} &= -\frac{\hat{a}_0 \mu^{2\epsilon}}{4} (\phi\phi)_0 (\phi\phi)_0 = -\frac{\hat{a}_0 \mu^{2\epsilon}}{4} (\phi_{ij} \phi_{ij}) (\phi_{kl} \phi_{kl}) = \\
&= -\frac{\hat{a}_0 \mu^{2\epsilon}}{4} (2(\phi_{12}^2 + \phi_{13}^2 + \phi_{14}^2 + \phi_{23}^2 + \phi_{24}^2 + \phi_{34}^2))^2 = \\
&= -\frac{\hat{a}_0 \mu^{2\epsilon}}{4} \left[4\phi_{12}^4 + 8\phi_{12}^2(\phi_{13}^2 + \phi_{14}^2 + \phi_{23}^2 + \phi_{24}^2 + \phi_{34}^2) + \right. \\
&\quad + 4\phi_{13}^4 + 8\phi_{13}^2(\phi_{14}^2 + \phi_{23}^2 + \phi_{24}^2 + \phi_{34}^2) + \\
&\quad + 4\phi_{14}^4 + 8\phi_{14}^2(\phi_{23}^2 + \phi_{24}^2 + \phi_{34}^2) + \\
&\quad + 4\phi_{23}^4 + 8\phi_{23}^2(\phi_{24}^2 + \phi_{34}^2) + \\
&\quad + 4\phi_{24}^4 + 8\phi_{24}^2(\phi_{34}^2) + \\
&\quad \left. + 4\phi_{34}^4 \right]. \tag{3.28}
\end{aligned}$$

The \hat{a}_2 -term in (3.15) yields

$$\begin{aligned}
\mathcal{L}_{\hat{a}_2} &= -\frac{\hat{a}_2 \mu^{2\epsilon}}{4} (\phi\phi)_2 (\phi\phi)_2 = -\frac{\hat{a}_2 \mu^{2\epsilon}}{4} (\phi_{ij} \phi_{ik}) (\phi_{lj} \phi_{lk}) = \\
&= -\frac{\hat{a}_2 \mu^{2\epsilon}}{4} \left[2(\phi_{12}^4 + \phi_{13}^4 + \phi_{14}^4 + \phi_{23}^4 + \phi_{24}^4 + \phi_{34}^4) \right. \\
&\quad + 4\phi_{12}^4(\phi_{13}^2 + \phi_{14}^2 + \phi_{23}^2 + \phi_{24}^2) + \\
&\quad + 4\phi_{13}^4(\phi_{14}^2 + \phi_{23}^2 + \phi_{34}^2) + \\
&\quad + 4\phi_{14}^4(\phi_{24}^2 + \phi_{34}^2) + \\
&\quad + 4\phi_{23}^4(\phi_{24}^2 + \phi_{34}^2) + \\
&\quad + 4\phi_{24}^4(\phi_{34}^2) + \\
&\quad \left. + 8\phi_{12}\phi_{13}\phi_{42}\phi_{43} + 8\phi_{12}\phi_{14}\phi_{32}\phi_{34} + 8\phi_{13}\phi_{14}\phi_{23}\phi_{24} \right]. \tag{3.29}
\end{aligned}$$

Note that the antisymmetry of the ϕ -fields has been utilized in the expressions

above.

By looking at the expressions (3.28) and (3.29) one can infer that for all 4-point functions there is a 1-loop contribution proportional to $\hat{a}_0\hat{a}_2$. Furthermore, if one considers any 4-point function with a 1-loop contribution proportional to \hat{a}_0^2 then there is a 1-loop contribution proportional to \hat{a}_2^2 . However, the 4-point function $\Gamma_{1loop}(\phi_{12}\phi_{13} \rightarrow \phi_{42}\phi_{43})$ only has 1-loop contribution proportional to \hat{a}_2^2 and to $\hat{a}_0\hat{a}_2$ but has no 1-loop contributions proportional to \hat{a}_0^2 . Therefore, one of the chosen Γ s will be $\Gamma^2 \equiv \Gamma(\phi_{12}\phi_{13} \rightarrow \phi_{42}\phi_{43})$. For simplicity, the other 4-point function will be chosen as $\Gamma^1 \equiv \Gamma(\phi_{12}\phi_{12} \rightarrow \phi_{12}\phi_{12})$.

In what follows, the 1-loop contribution to a 4-point function $\Gamma_{1loop}(\phi_1\phi_2 \rightarrow \phi_3\phi_4)$ proportional to $\hat{a}_i\hat{a}_j$ will be denoted by $\Gamma_{1loop}^{\hat{a}_i\hat{a}_j}(\phi_1\phi_2 \rightarrow \phi_3\phi_4)$.

To summarize, the counterterm fixing conditions now read

$$\begin{aligned} &\Gamma_{1loop}(\phi_{12}\phi_{12} \rightarrow \phi_{12}\phi_{12}) + \Gamma_{Ka0}(\phi_{12}\phi_{12} \rightarrow \phi_{12}\phi_{12}) \\ &\quad + \Gamma_{Ka2}(\phi_{12}\phi_{12} \rightarrow \phi_{12}\phi_{12}) \stackrel{!}{=} \text{finite} \\ &\Gamma_{1loop}(\phi_{12}\phi_{13} \rightarrow \phi_{42}\phi_{43}) + \Gamma_{Ka0}(\phi_{12}\phi_{13} \rightarrow \phi_{42}\phi_{43}) \\ &\quad + \Gamma_{Ka2}(\phi_{12}\phi_{13} \rightarrow \phi_{42}\phi_{43}) \stackrel{!}{=} \text{finite}. \end{aligned} \tag{3.30}$$

For the 1-loop contributions then holds

$$\begin{aligned} \Gamma_{1loop}(\phi_{12}\phi_{12} \rightarrow \phi_{12}\phi_{12}) &= \Gamma_{1loop}^{\hat{a}_0^2}(\phi_{12}\phi_{12} \rightarrow \phi_{12}\phi_{12}) + \Gamma_{1loop}^{\hat{a}_0\hat{a}_2}(\phi_{12}\phi_{12} \rightarrow \phi_{12}\phi_{12}) \\ &\quad + \Gamma_{1loop}^{\hat{a}_2^2}(\phi_{12}\phi_{12} \rightarrow \phi_{12}\phi_{12}) + \Gamma_{1loop}^{\hat{g}^4}(\phi_{12}\phi_{12} \rightarrow \phi_{12}\phi_{12}) \\ \Gamma_{1loop}(\phi_{12}\phi_{13} \rightarrow \phi_{42}\phi_{43}) &= \Gamma_{1loop}^{\hat{a}_0\hat{a}_2}(\phi_{12}\phi_{13} \rightarrow \phi_{42}\phi_{43}) + \Gamma_{1loop}^{\hat{a}_2^2}(\phi_{12}\phi_{13} \rightarrow \phi_{42}\phi_{43}) \\ &\quad + \Gamma_{1loop}^{\hat{g}^4}(\phi_{12}\phi_{13} \rightarrow \phi_{42}\phi_{43}). \end{aligned} \tag{3.31}$$

Note that in the expressions for the 4-point functions above also appeared 1-loop contributions proportional to \hat{g}^4 . These contributions also have to be accounted for because the interaction term (3.51) does in fact produce diagrams of the type $\phi_1\phi_2 \rightarrow \phi_3\phi_4$ (where the loop is made out of gauge fields).

In the following subsections the contributions to the 4-point functions in (3.30) will be evaluated. It is worth to point out that only the pole terms of the 1-loop contributions will be necessary to compute since the MS scheme is being employed. With these expressions at hand the counterterms K_{a_0} and K_{a_2} will be determined and plugged into (3.20). This way the contribution of the K -terms to the beta function will be obtained. Thus, together with the result (3.26) this will mean that the running of the scalar couplings a_0 and a_2 in the $SO(4)$ Higgs model will be fully determined.

3.4.1 Purely scalar contributions to $\Gamma(\phi_{12}\phi_{12} \rightarrow \phi_{12}\phi_{12})$

To start off, the contributions to $\Gamma_{1loop}(\phi_{12}\phi_{12} \rightarrow \phi_{12}\phi_{12})$ proportional to \hat{a}_0^2 will be evaluated, i.e. the term $\Gamma_{1loop}^{\hat{a}_0^2}(\phi_{12}\phi_{12} \rightarrow \phi_{12}\phi_{12})$. Looking at (3.28), one can infer that all of the contributing Feynman diagrams are the ones depicted in Figure 3.4. Note that the pairs of indices of the fields are written down in

the ascending order, which automatically includes the other way of ordering the indices since the ϕ -fields are antisymmetric.

When it comes to evaluating $\Gamma_{1loop}^{\hat{a}_0^2}(\phi_{12}\phi_{12} \rightarrow \phi_{12}\phi_{12})$, there are two steps - evaluation of the integral coming from the loops and the computation of the combinatorial factor coming from the number of possible contractions of the fields as well as from the number of summands in (3.28).

First, the evaluation of the integral will be discussed. In order to compute the integral only the structure of the diagram shown in Figure 3.5 is needed. The corresponding Feynman rules for the scalar loop are specified in Figure 3.6.

Utilizing the Feynman rules, the contribution corresponding to the diagram in Figure 3.5 will have the form

$$iI_{sc} = P \left(-i \frac{\hat{a}_0}{4} \right)^2 \mu^{2\epsilon} \frac{1}{2} \int \frac{d^d l}{(2\pi)^d} \frac{i^2}{(l^2 - m^2)((l+p)^2 - m^2)}, \quad (3.32)$$

where the regularization parameter μ popped up as necessary within the dimensional regularization scheme. The factor $\frac{1}{2}$ is there because the graphs correspond to the second order of the Dyson expansion and the factor P denotes all the combinatorial factors which appear due to the various ways of how to contract the fields - this will be discussed in detail later on. Now, the Feynman parametrization (B.1) will be introduced into the integral in (3.32) and the relation (B.2) will be utilized which yields

$$\begin{aligned} \int \frac{d^d l}{(2\pi)^d} \frac{1}{(l^2 - m^2)((l+p)^2 - m^2)} &= \int \frac{d^d l}{(2\pi)^d} \int_0^1 dx \frac{1}{(l^2 - C)^2} = \\ &= \int_0^1 dx (-1)^2 i \frac{1}{(4\pi)^{d/2}} C^{-\epsilon} \frac{\Gamma(2-\epsilon)\Gamma(\epsilon)}{\Gamma(2-\epsilon)\Gamma(2)} = \frac{i}{16\pi^2\epsilon} + (O(1)). \end{aligned} \quad (3.33)$$

In the expressions above there was denoted $C = p^2 x^2 - xp^2 + m^2$, in the second equality there was used the DR master formula (B.2) and in the last equality there was employed the Taylor expansion of the whole expression where for the Gamma function holds

$$\Gamma(\epsilon) = \frac{1}{\epsilon} - \gamma_E + O(\epsilon), \quad (3.34)$$

where $\gamma_E \approx 0.577$ is the Euler-Mascheroni constant. Plugging the resulting integral into (3.32) means for the divergent part

$$I_{sc}^{div} = P \frac{\hat{a}_0^2}{32} \mu^{2\epsilon} \frac{1}{16\pi^2\epsilon} + O(1). \quad (3.35)$$

As was mentioned in the previous section the MS scheme is being utilized, therefore only the pole the term of I_{sc} was evaluated.

Having evaluated the integral part of $\Gamma_{1loop}^{\hat{a}_0^2}(\phi_{12}\phi_{12} \rightarrow \phi_{12}\phi_{12})$ now it is necessary to calculate the combinatorial factors for the diagrams in Figure 3.4. There are two different types of diagrams when it comes to the combinatorial factors and those are: a diagram where the loop is made of $\phi_{12}\phi_{12}$ (the first diagram in

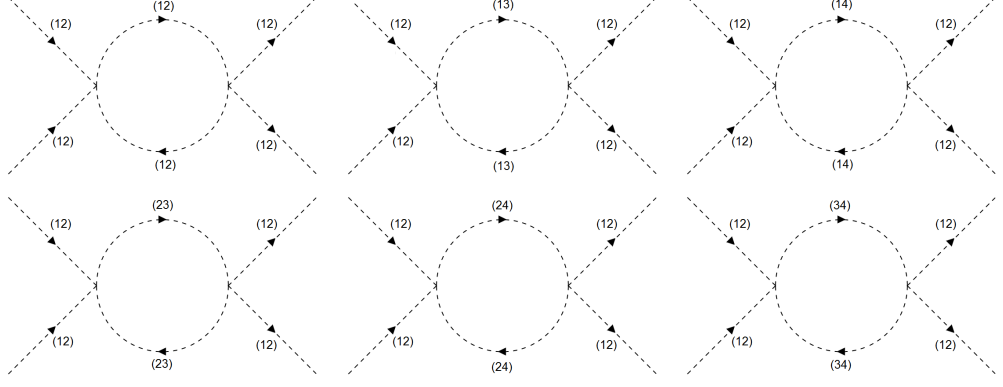


Figure 3.4: 1-loop diagrams contributing to $\Gamma_{1loop}^{\hat{a}_0^2}(\phi_{12}\phi_{12} \rightarrow \phi_{12}\phi_{12})$. The pairs of numbers next to the scalar lines denote the particular scalar fields.

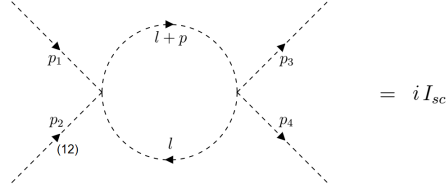


Figure 3.5: A purely scalar 1-loop diagram.

Figure 3.4) and then the rest of the diagrams. For the first diagram the combinatorial factor has $f_{\mathcal{L}} = 4^2$ for the factors in (3.28)³, for the contractions there are $f_l = \binom{4}{2}\binom{4}{2}2$ ways of how to construct a loop and then there are $f_o = 4!$ ways of how to connect the outer legs, so together the combinatorial factor is equal to $f_d = f_{\mathcal{L}} \times f_l \times f_o = 4^2 \times \binom{4}{2}\binom{4}{2}2 \times 4! = 27648$. For the other diagrams (where the loop is made of fields other than ϕ_{12}) the combinatorial factor has $f_{\mathcal{L}} = 8^2$, for the contractions there are $f_l = \binom{2}{2}\binom{2}{2}2$ ways of how to construct the loop, there are $f_o = 4!$ ways of how to contract the outer legs, and there are $n_d = 5$ of those diagrams, so together the combinatorial factor is equal to $f_d = f_{\mathcal{L}} \times f_l \times f_o \times n_d = 8^2 \times \binom{2}{2}\binom{2}{2}2 \times 4! \times 5 = 15360$. Altogether, these numbers form the total combinatorial factor

$$P_1^{\hat{a}_0^2} = 27648 + 15360 = 43008, \quad (3.36)$$

where the subscript 1 means that it corresponds to the contribution to the 4-point function $\Gamma^1 \equiv \Gamma(\phi_{12}\phi_{12} \rightarrow \phi_{12}\phi_{12})$.

When the integral part together with the combinatorial part are put together,

³In order to make the calculations of the combinatorial factors more transparent the following notation will be used throughout the thesis: $f_{\mathcal{L}}$ = (product of the factors coming out of the interaction terms in the Lagrangian); f_l = (number of ways of how to contract the fields in order to construct a loop); f_o = (number of ways of how to connect the outer legs to the loop); n_d = (number of the specified set of diagrams); f_d = (the overall combinatorial factor for the specified set of diagrams)

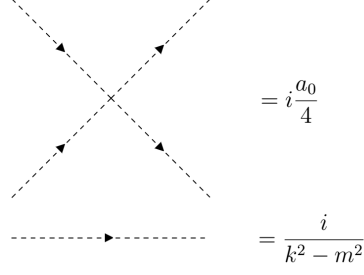


Figure 3.6: Feynman rules for the scalar vertex and the scalar propagator.

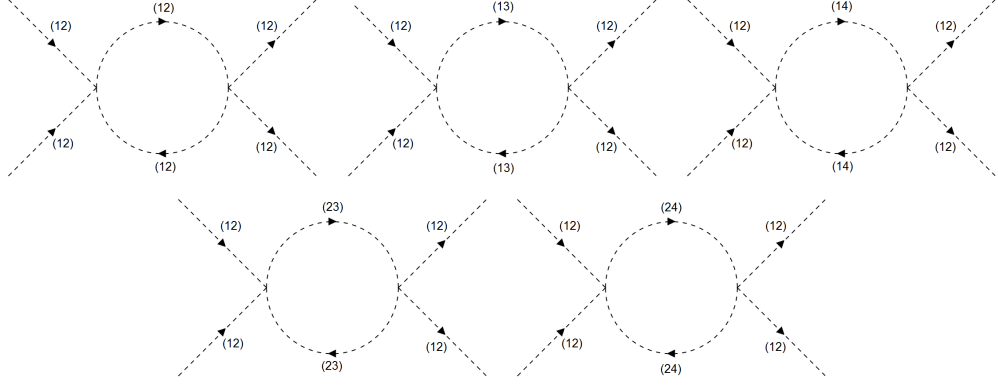


Figure 3.7: 1-loop diagrams contributing to $\Gamma_{1loop}^{\hat{a}_2^2}(\phi_{12}\phi_{12} \rightarrow \phi_{12}\phi_{12})$.

the total contribution reads

$$\begin{aligned}
 \Gamma_{1loop}^{\hat{a}_0^2}(\phi_{12}\phi_{12} \rightarrow \phi_{12}\phi_{12}) &= P_1^{a_0^2} \left(-i \frac{\hat{a}_0}{4} \right)^2 \mu^{2\epsilon} \frac{1}{2} \int \frac{d^d l}{(2\pi)^d} \frac{i^2}{(l^2 - m^2)((l+p)^2 - m^2)} = \\
 &= 43008 \frac{\hat{a}_0^2}{32} \mu^{2\epsilon} \frac{1}{16\pi^2 \epsilon}.
 \end{aligned} \tag{3.37}$$

Now the contributions to $\Gamma_{1loop}(\phi_{12}\phi_{12} \rightarrow \phi_{12}\phi_{12})$ proportional to \hat{a}_2^2 shall be evaluated, i.e. the term $\Gamma_{1loop}^{\hat{a}_2^2}(\phi_{12}\phi_{12} \rightarrow \phi_{12}\phi_{12})$. Looking at \mathcal{L}_{a_2} in (3.29), all of the contributing diagrams are the ones depicted in Figure 3.7.

As was the case for the part proportional to a_0^2 , the calculation here has two parts - the integral part and the combinatorial part. However, since the structure of the scalar loop remains the same, the result of the integration will also be the same, thus only the combinatorial part has to be computed.

The first diagram in 3.7 which has the loop made of ϕ_{12} receives the factor $f_{\mathcal{L}} = 2^2$ coming out of the Lagrangian (3.29), then there are $f_l \times f_o = \binom{4}{2} \binom{4}{2} 2 \times 4!$ number of possible contractions (as was the case for the a_0^2 proportional part), thus altogether the relevant factor is equal to $f_d = f_{\mathcal{L}} \times f_l \times f_o = 2^2 \times \binom{4}{2} \binom{4}{2} 2 \times 4! = 6912$. For the rest of the diagrams together - the combinatorial factor receives $f_{\mathcal{L}} = 4^2$, there are $f_l \times f_o = \binom{2}{2} \binom{2}{2} 2 \times 4!$ possible contractions, and there are $n_d = 4$ of such diagrams, hence the factor for the diagrams is equal to $f_d = f_{\mathcal{L}} \times f_l \times f_o \times n_d = 4^2 \times \binom{2}{2} \binom{2}{2} 2 \times 4! \times 4 = 3072$. Putting all of the factors

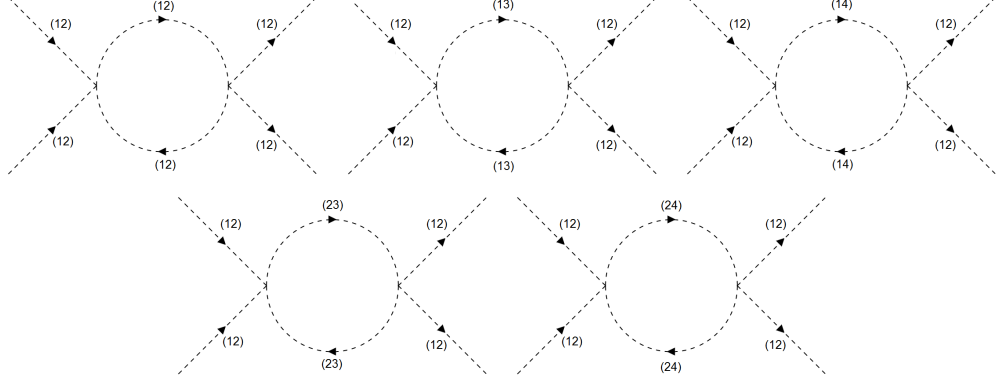


Figure 3.8: 1-loop diagrams contributing to $\Gamma_{1loop}^{\hat{a}_0\hat{a}_2}(\phi_{12}\phi_{12} \rightarrow \phi_{12}\phi_{12})$.

together, the overall combinatorial factor has the form

$$P_1^{\hat{a}_2^2} = 6912 + 3072 = 9984. \quad (3.38)$$

This means that the contribution to $\Gamma_{1loop}(\phi_{12}\phi_{12} \rightarrow \phi_{12}\phi_{12})$ proportional to \hat{a}_2^2 is

$$\Gamma_{1loop}^{\hat{a}_2^2}(\phi_{12}\phi_{12} \rightarrow \phi_{12}\phi_{12}) = 9984 \frac{\hat{a}_2^2}{32} \mu^{2\epsilon} \frac{1}{16\pi^2\epsilon}. \quad (3.39)$$

Next, the diagrams proportional to $\hat{a}_0\hat{a}_2$ will be computed. The term in the Dyson series responsible for these contributions is proportional to

$$\mathcal{L}_{a_0}(x)\mathcal{L}_{a_2}(y) + \mathcal{L}_{a_0}(y)\mathcal{L}_{a_2}(x) \quad (3.40)$$

and by evaluating the expression, one arrives at the diagrams shown in Figure 3.8.

The integral part of the computation remains the same as in the previous cases. For the first diagram in 3.8 the combinatorial factor has 2 for the permutation of vertices $x \leftrightarrow y$ and there is a factor of 4×2 from (3.28) and (3.29) resulting in $f_{\mathcal{L}} = 2 \times 4 \times 2$; $f_l \times f_o = \binom{4}{2}\binom{4}{2}2 \times 4!$ is the factor coming out of the contractions, so altogether the factor is equal to $f_d = f_{\mathcal{L}} \times f_l \times f_o = 2 \times 4 \times 2 \times \binom{4}{2}\binom{4}{2}2 \times 4! = 27648$. For the rest of the diagrams in 3.8, there is factor of 2 for the permutation of vertices $x \leftrightarrow y$, there is a factor $4 * 8$ coming from (3.28) and (3.29) which means $f_{\mathcal{L}} = 2 \times 4 \times 8$, there are $f_l \times f_o = \binom{2}{2}\binom{2}{2}2 \times 4!$ possible contractions, and there are $n_d = 4$ such diagrams, hence the overall factor is equal to $f_d = f_{\mathcal{L}} \times f_l \times f_o \times n_d = 2 \times 4 \times 8 \times \binom{2}{2}\binom{2}{2}2 \times 4! \times 4 = 12288$. The overall factor is thus equal to

$$P_1^{\hat{a}_0\hat{a}_2} = 27648 + 12288 = 39936, \quad (3.41)$$

which means the contribution to $\Gamma_{1loop}(\phi_{12}\phi_{12} \rightarrow \phi_{12}\phi_{12})$ proportional to $\hat{a}_0\hat{a}_2$ is

$$\Gamma_{1loop}^{\hat{a}_0\hat{a}_2}(\phi_{12}\phi_{12} \rightarrow \phi_{12}\phi_{12}) = 39936 \frac{\hat{a}_0\hat{a}_2}{32} \mu^{2\epsilon} \frac{1}{16\pi^2\epsilon}. \quad (3.42)$$

Having computed the 1-loop contributions, now it is necessary to calculate the contributions of the counterterms $\Gamma_{K_{a_0}}(\phi_{12}\phi_{12} \rightarrow \phi_{12}\phi_{12})$ and $\Gamma_{K_{a_2}}(\phi_{12}\phi_{12} \rightarrow \phi_{12}\phi_{12})$. The diagrams corresponding to K_{a_0} and to K_{a_2} are shown in Figure 3.3. Note that the graphs have an identical structure, the only difference comes from the combinatorial factors. The explicit form of the interaction terms corresponding to the counterterms are the same as the ones in (3.28) and (3.29), with the only difference being the multiplicative constant $\hat{a}_i \rightarrow \hat{a}_i K_{a_i}$.

The contribution of the K_{a_0} -term receives a factor of $f_{\mathcal{L}} = 4$ from (3.28) and a factor of $f_o = 4!$ for the contractions. Thus, the overall combinatorial factor has the form

$$P_1^{K_{a_0}} = f_{\mathcal{L}} \times f_o = 4 \times 4! = 96. \quad (3.43)$$

Similarly, the contribution of the K_{a_2} has the factor of $f_{\mathcal{L}} = 2$ from (3.29) and $f_o = 4!$ for the contractions. Therefore, the total combinatorial factor reads

$$P_1^{K_{a_2}} = f_{\mathcal{L}} \times f_o = 2 \times 4! = 48, \quad (3.44)$$

When put together, the overall contributions of the counterterms to the 4-point function $\Gamma(\phi_{12}\phi_{12} \rightarrow \phi_{12}\phi_{12})$ are

$$\begin{aligned} \Gamma_{K_{a_0}}(\phi_{12}\phi_{12} \rightarrow \phi_{12}\phi_{12}) &= -96\mu^{2\epsilon} \frac{\hat{a}_0 K_{a_0}}{4} \\ \Gamma_{K_{a_2}}(\phi_{12}\phi_{12} \rightarrow \phi_{12}\phi_{12}) &= -48\mu^{2\epsilon} \frac{\hat{a}_2 K_{a_2}}{4}. \end{aligned} \quad (3.45)$$

3.4.2 Purely scalar contributions to $\Gamma(\phi_{12}\phi_{13} \rightarrow \phi_{42}\phi_{43})$

First, the term $\Gamma_{1loop}^{\hat{a}_2^2}(\phi_{12}\phi_{13} \rightarrow \phi_{42}\phi_{43})$ will be determined which means it is necessary to compute the contributions to $\Gamma_{1loop}(\phi_{12}\phi_{13} \rightarrow \phi_{42}\phi_{43})$ proportional to \hat{a}_2^2 . Note that in this section there is an exception to the convention of keeping the indices in the ascending order in the cases of ϕ_{42} and ϕ_{43} (which is a bit more convenient choice when looking at the index structure of the a_2 term). Of course this choice of ordering makes no difference whatsoever as long as the combinatorial factors are evaluated properly.

Looking at the interaction terms in (3.29) one can infer that all of the relevant diagrams are the ones depicted in Figure 3.9.

The computation of $\Gamma_{1loop}^{\hat{a}_2^2}(\phi_{12}\phi_{13} \rightarrow \phi_{42}\phi_{43})$ again has two parts - the integral one and the combinatorial one. However, the integral part is obviously the same as in the case of $\Gamma_{1loop}(\phi_{12}\phi_{12} \rightarrow \phi_{12}\phi_{12})$. This means that the 1-loop contribution to the 4-point function proportional to \hat{a}_2^2 is given by eq. (3.35).

Now the combinatorial part of the computation of $\Gamma_{1loop}^{\hat{a}_2^2}(\phi_{12}\phi_{13} \rightarrow \phi_{42}\phi_{43})$ shall be presented. The first four diagrams in Figure 3.9 receive a factor of 2 for the permutation of vertices $x \leftrightarrow y$, then there is 4×8 from the factors in (3.29) which means $f_{\mathcal{L}} = 2 \times 4 \times 8$; as for the contraction there are $f_l = \binom{2}{1} \binom{2}{1}$ ways of how to construct a loop and $f_o = 1$; there are $n_d = 4$ of those diagrams; thus,

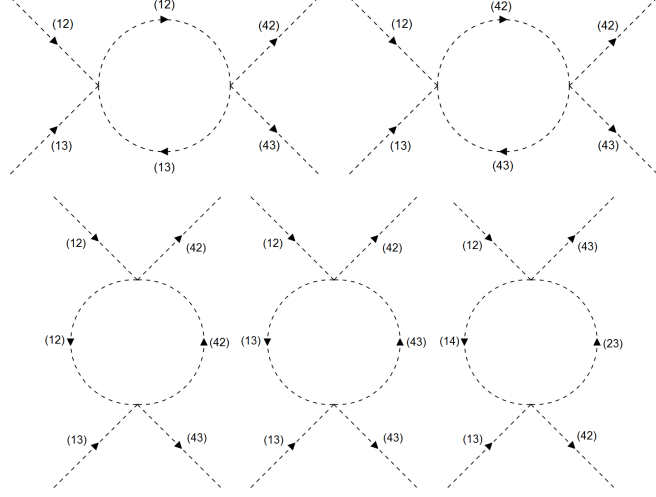


Figure 3.9: 1-loop diagrams contributing to $\Gamma_{1loop}^{\hat{a}_2^2}(\phi_{12}\phi_{13} \rightarrow \phi_{42}\phi_{43})$.

the overall factor is $f_d = f_{\mathcal{L}} \times f_l \times f_o \times n_d = 2 \times 4 \times 8 \times \binom{2}{1} \binom{2}{1} \times 4 = 1024$. The last diagram in Figure 3.9 has a factor of 2 for the permutation of vertices, then it receives $8 * 8$ from the factors (3.29) so $f_{\mathcal{L}} = 2 \times 8 \times 8$ and crucially there is a factor of $(-1)^3$ responsible for the permutation of the subscripts of the ϕ -fields, hence the overall factor is equal to $f_d = 2 \times 8 \times 8 \times (-1)^3 = -128$. The overall combinatorial factor has the form

$$P_2^{\hat{a}_2^2} = 1024 - 128 = 896, \quad (3.46)$$

which means the contribution to $\Gamma_{1loop}(\phi_{12}\phi_{13} \rightarrow \phi_{42}\phi_{43})$ proportional to \hat{a}_2^2 is

$$\Gamma_{1loop}^{\hat{a}_2^2}(\phi_{12}\phi_{13} \rightarrow \phi_{42}\phi_{43}) = 896 \frac{\hat{a}_2^2}{32} \mu^{2\epsilon} \frac{1}{16\pi^2\epsilon}. \quad (3.47)$$

Another contribution to $\Gamma_{1loop}(\phi_{12}\phi_{13} \rightarrow \phi_{42}\phi_{43})$ is the one proportional to $\hat{a}_0\hat{a}_2$, which again comes from the term $\mathcal{L}_{a_0}(x)\mathcal{L}_{a_2}(y) + \mathcal{L}_{a_0}(y)\mathcal{L}_{a_2}(x)$. After carrying out the multiplication of all the terms it is easy to see that the diagrams contributing to $\Gamma_{1loop}^{\hat{a}_0\hat{a}_2}(\phi_{12}\phi_{13} \rightarrow \phi_{42}\phi_{43})$ are the ones depicted in Figure 3.10.

The structure of all of the diagrams in Figure 3.10 is very similar meaning that the combinatorial factors for all of the graphs are the same. In particular, there is a factor of 2 for the permutation of the vertices, there is 8×8 from the factors in (3.28) and (3.29) which means $f_{\mathcal{L}} = 2 \times 8 \times 8$, there are $f_l = \binom{2}{1} \binom{2}{1}$ ways of how to construct a loop, and there are $n_d = 6$ of the diagrams. Put together, the overall factor has the form

$$P_2^{\hat{a}_0\hat{a}_2} = f_{\mathcal{L}} \times f_l \times n_d = 2 \times 8 \times 8 \times \binom{2}{1} \binom{2}{1} \times 6 = 3072, \quad (3.48)$$

which means the contribution to $\Gamma_{1loop}(\phi_{12}\phi_{13} \rightarrow \phi_{42}\phi_{43})$ proportional to $\hat{a}_0\hat{a}_2$ is

$$\Gamma_{1loop}^{\hat{a}_0\hat{a}_2}(\phi_{12}\phi_{13} \rightarrow \phi_{42}\phi_{43}) = 3072 \frac{\hat{a}_0\hat{a}_2}{32} \mu^{2\epsilon} \frac{1}{16\pi^2\epsilon}. \quad (3.49)$$

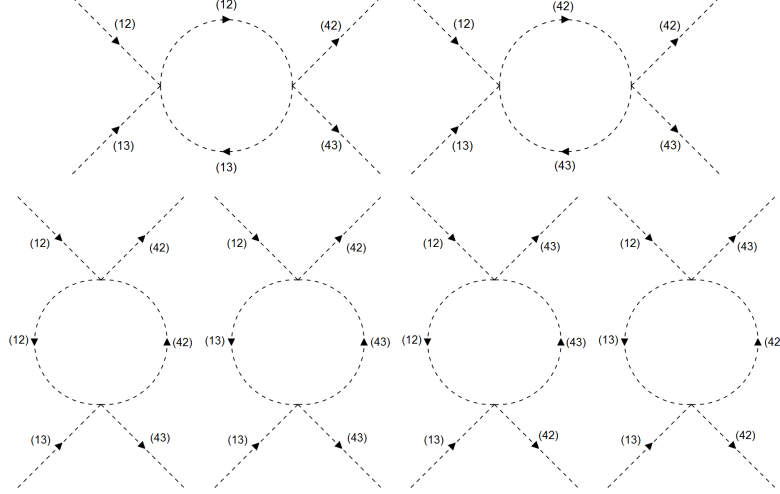


Figure 3.10: 1-loop diagrams contributing to $\Gamma_{1loop}^{\hat{a}_0 \hat{a}_2}(\phi_{12}\phi_{13} \rightarrow \phi_{42}\phi_{43})$.

As was mentioned earlier, the contribution $\Gamma_{1loop}^{\hat{a}_0^2}(\phi_{12}\phi_{13} \rightarrow \phi_{42}\phi_{43})$ vanishes since there is now way to produce a 1-loop diagram of $\phi_{12}\phi_{13} \rightarrow \phi_{42}\phi_{43}$ using only the a_0 -term in eq. (3.28).

Now it is necessary to evaluate the contributions of the counterterms to $\Gamma(\phi_{12}\phi_{13} \rightarrow \phi_{42}\phi_{43})$ which pictorially look like the one in Figure 3.3. However, the contribution proportional to K_{a_0} vanishes since the interaction term fails to produce tree graphs of the form $\phi_{12}\phi_{13} \rightarrow \phi_{42}\phi_{43}$. The contribution to $\Gamma(\phi_{12}\phi_{13} \rightarrow \phi_{42}\phi_{43})$ proportional to K_{a_2} only receives a factor of 8 from (3.29), thus it has the form

$$\Gamma_{1loop}^{Ka_2}(\phi_{12}\phi_{13} \rightarrow \phi_{42}\phi_{43}) = -8\mu^{2\epsilon} \frac{\hat{a}_2 K_{a_2}}{4}. \quad (3.50)$$

3.4.3 Contributions to Γ^1 and to Γ^2 proportional to \hat{g}^4

All of the 1-loop contributions to $\Gamma^1 \equiv \Gamma(\phi_{12}\phi_{12} \rightarrow \phi_{12}\phi_{12})$ and to $\Gamma^2 \equiv \Gamma(\phi_{12}\phi_{13} \rightarrow \phi_{42}\phi_{43})$ proportional to \hat{g}^4 come from the term containing covariant derivatives in (3.15). Namely, the relevant interaction terms are of the $\phi\phi AA$ type and they read

$$i(-i)\frac{1}{4}\hat{g}^2\mu^{2\epsilon} [A_\mu, \phi]_{ij}^\dagger [A_\mu, \phi]_{ij} = \frac{1}{4}\hat{g}^2\mu^{2\epsilon} (A^{ik} A^{il} \phi_{kj} \phi_{lj} + A^{ik} A^{jl} \phi_{kj} \phi_{il}). \quad (3.51)$$

Since the full expansion of the expression above is a bit lengthy it is deferred to Appendix C.

To begin with, the 1-loop contributions to $\Gamma(\phi_{12}\phi_{12} \rightarrow \phi_{12}\phi_{12})$ proportional to \hat{g}^4 will be evaluated. The corresponding Feynman diagrams are depicted in Figure 3.11.

As before, the evaluation of the diagrams in Figure 3.11 has two parts - the integral part and the combinatorial part. Obviously, all of the diagrams in Figure

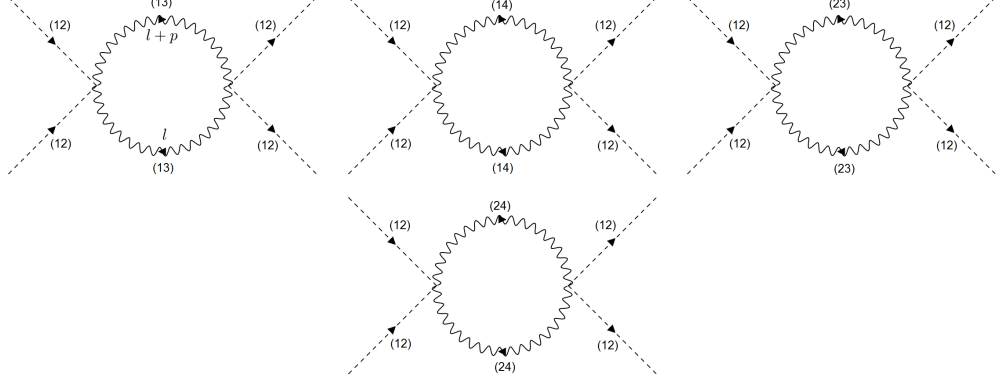


Figure 3.11: Contributions to $\Gamma_{1loop}^{\hat{g}^4}(\phi_{12}\phi_{12} \rightarrow \phi_{12}\phi_{12})$. For the momenta it holds $p = p_1 + p_2$.

3.11 produce the same integral which has the form (the momenta are given in the first graph in the Figure)

$$\Gamma_{1loop}^{\hat{g}^4}(\phi_{12}\phi_{12} \rightarrow \phi_{12}\phi_{12}) = P \left(-\frac{i\hat{g}^4}{4} \right)^2 \mu^{2\epsilon} \frac{1}{2} \int \frac{d^d l}{(2\pi)^d} g_{\mu\rho} g_{\nu\sigma} D^{\mu\nu}(l) D^{\rho\sigma}(l+p). \quad (3.52)$$

In the expression above the vector boson propagator was denoted by $D^{\mu\nu}(l)$ and its form was given in eq. (3.23). The factor P in (3.52) stands for a generic combinatorial factor. After performing the standard procedure of introducing the Feynman parameters (B.1) and utilizing the DR master formula (B.2) the expression (3.52) reads

$$\Gamma_{1loop}^{\hat{g}^4}(\phi_{12}\phi_{12} \rightarrow \phi_{12}\phi_{12}) = P \frac{\hat{g}^4}{32} \mu^{2\epsilon} \frac{3}{16\pi^2\epsilon}. \quad (3.53)$$

The second part of evaluating graphs in Figure 3.11 comes down to the combinatorial factors. The factors are the same for all of the diagrams and they contain a factor of $f_{\mathcal{L}} = 1$ from (C.3), then there are $f_l = 2$ ways of how to construct a loop, and there are $f_o = 4!$ ways of how to connect the outer legs. Thus the total factor is equal to

$$P_1^{\hat{g}^4} = 1 \times 2 \times 4! \times 4 = 192 \quad (3.54)$$

Put altogether the 1-loop contribution to $\Gamma(\phi_{12}\phi_{12} \rightarrow \phi_{12}\phi_{12})$ proportional to \hat{g}^4 is

$$\Gamma_{1loop}^{\hat{g}^4}(\phi_{12}\phi_{12} \rightarrow \phi_{12}\phi_{12}) = 192 \frac{\hat{g}^4}{32} \mu^{2\epsilon} \frac{3}{16\pi^2\epsilon}. \quad (3.55)$$

The 1-loop diagrams contributing to $\Gamma(\phi_{12}\phi_{13} \rightarrow \phi_{42}\phi_{43})$ proportional to \hat{g}^4 are depicted in Figure 3.12. From the interaction terms in (C.4)-(C.9) can be inferred that the first four diagrams in Figure 3.12 receive the same factor $2 \times (-2)$ and then there is a factor of 2 for the permutation of vertices so $f_{\mathcal{L}} = 2 \times (-2) \times 2$, which

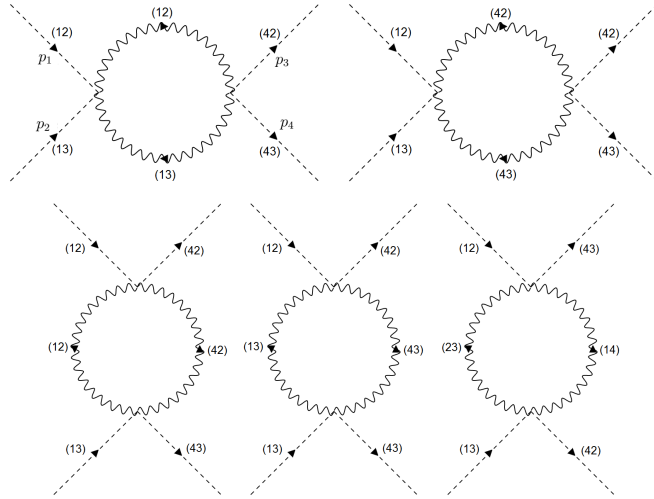


Figure 3.12: Contributions to $\Gamma_{1loop}^{\hat{g}^4}(\phi_{12}\phi_{13} \rightarrow \phi_{42}\phi_{43})$.

together gives the factor $f_d = f_{\mathcal{L}} \times n_d = 2 \times (-2) \times 2 \times 4 = -32$. The last diagram in Figure 3.12 receives a factor of $4 \times (-4)$ from (C.6) and (C.7) and a factor of 2 for the permutation of vertices, which means that $f_d = 4 \times (-4) \times 2 = -32$. The overall factor is then equal to

$$P_2^{\hat{g}^4} = -32 - 32 = -64, \quad (3.56)$$

which means the 1-loop contribution to $\Gamma(\phi_{12}\phi_{13} \rightarrow \phi_{42}\phi_{43})$ proportional to \hat{g}^4 is

$$\Gamma_{1loop}^{\hat{g}^4}(\phi_{12}\phi_{13} \rightarrow \phi_{42}\phi_{43}) = -64 \frac{\hat{g}^4}{32} \mu^{2\epsilon} \frac{3}{16\pi^2\epsilon}. \quad (3.57)$$

It is necessary to observe that the diagrams presented in this subsection have not exhausted the full list of 1-loop diagrams with gauge fields potentially contributing to $\Gamma(\phi_{12}\phi_{12} \rightarrow \phi_{12}\phi_{12})$ or to $\Gamma(\phi_{12}\phi_{13} \rightarrow \phi_{42}\phi_{43})$. Those 4-point functions may in fact have other contributing 1-loop diagrams proportional to \hat{g}^4 or to $\hat{g}^2 \hat{a}_i$ whose structure is depicted in Figure 3.13. However, all of these diagrams turn out to be in fact finite. This observation can be shown by counting the superficial degree of divergence α , which in this case can be defined as

$$\alpha = 4L - 2B + \sum_i n_i d_i, \quad (3.58)$$

where L is the number of loops, B is the number of internal bosonic lines, n_i is the number of i -th vertices and d_i is the number of derivatives associated to the i -th vertex.

One can observe that if for a diagram in Figure 3.13 $\alpha = 0$, then the diagram is (potentially) logarithmically divergent. Recall the Feynman rule for the vertex depicted in 3.1 carries the factor of $(l + (\text{other momenta}))$ but only the l -proportional part contributes the divergent part of the diagram. This in turn means it is in fact irrelevant which of the ϕ -fields in a vertex (see (3.22)) is being taken the derivative of (regarding the divergent part of the diagram).

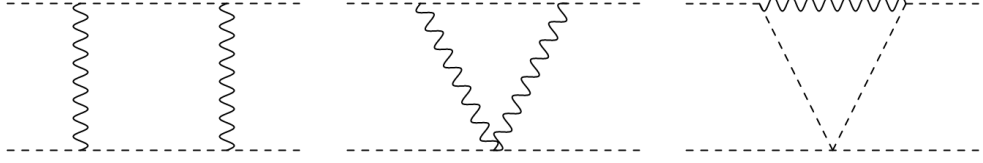


Figure 3.13: Diagrams with gauge fields with potentially non-trivial pole terms contributing to $\Gamma(\phi_{12}\phi_{12} \rightarrow \phi_{12}\phi_{12})$ or to $\Gamma(\phi_{12}\phi_{13} \rightarrow \phi_{42}\phi_{43})$.

This makes the interaction term (3.22) effectively symmetric with respect to the ϕ -fields sandwiching the generator, when one only cares about the divergent part of the diagram. However, since the generator is antisymmetric, the whole contribution of the vertex vanishes.

By looking at the diagrams in Figure 3.13 it is easy to infer that for all of them $\alpha = 0$. Also, all of these diagrams contain the triple vertex from the interaction term (3.22). Hence, due to the observations presented in the previous paragraph the divergent parts of the diagrams in Figure 3.13 vanish.

3.5 Beta functions of the couplings a_0 and a_2 in $SO(4)$ Higgs model

The beta functions of the couplings a_0 and a_2 are given by eq. (3.20) where one needs to plug in the K -terms as well as the wave-function renormalization factor. The latter of the two has been evaluated in sec. 4.3. and the result is given by (3.26) which is reiterated here for the reader's convenience

$$\Delta Z_\phi = \hat{g}^2 C_2(\text{Adj.}) \frac{3}{16\pi^2 \epsilon}. \quad (3.59)$$

As for the K -terms, these are determined via the equations (3.30) and (3.31). All of the terms in those equations have been calculated in sec.4.4 and for the reader's convenience they are summarized below

$$\begin{aligned} \Gamma_{1loop}^{\hat{a}_0^2}(\phi_{12}\phi_{12} \rightarrow \phi_{12}\phi_{12}) &= 43008 \frac{\hat{a}_0^2}{32} \mu^{2\epsilon} \frac{1}{16\pi^2 \epsilon} \\ \Gamma_{1loop}^{\hat{a}_2^2}(\phi_{12}\phi_{12} \rightarrow \phi_{12}\phi_{12}) &= 9984 \frac{\hat{a}_2^2}{32} \mu^{2\epsilon} \frac{1}{16\pi^2 \epsilon} \\ \Gamma_{1loop}^{\hat{a}_0 \hat{a}_2}(\phi_{12}\phi_{12} \rightarrow \phi_{12}\phi_{12}) &= 39936 \frac{\hat{a}_0 \hat{a}_2}{32} \mu^{2\epsilon} \frac{1}{16\pi^2 \epsilon} \\ \Gamma_{Ka0}(\phi_{12}\phi_{12} \rightarrow \phi_{12}\phi_{12}) &= -96 \mu^{2\epsilon} \frac{\hat{a}_0 K_{\hat{a}_0}}{4} \\ \Gamma_{Ka2}(\phi_{12}\phi_{12} \rightarrow \phi_{12}\phi_{12}) &= -48 \mu^{2\epsilon} \frac{\hat{a}_2 K_{\hat{a}_2}}{4} \\ \Gamma_{1loop}^{\hat{a}_2^2}(\phi_{12}\phi_{13} \rightarrow \phi_{42}\phi_{43}) &= 896 \frac{\hat{a}_2^2}{32} \mu^{2\epsilon} \frac{1}{16\pi^2 \epsilon} \end{aligned} \quad (3.60)$$

$$\begin{aligned}
\Gamma_{1loop}^{\hat{a}_0\hat{a}_2}(\phi_{12}\phi_{13} \rightarrow \phi_{42}\phi_{43}) &= 3072 \frac{\hat{a}_0\hat{a}_2}{32} \mu^{2\epsilon} \frac{1}{16\pi^2\epsilon} \\
\Gamma_{1loop}^{Ka_2}(\phi_{12}\phi_{13} \rightarrow \phi_{42}\phi_{43}) &= -8\mu^{2\epsilon} \frac{\hat{a}_2 K_{\hat{a}_2}}{4} \\
\Gamma_{1loop}^{\hat{g}^4}(\phi_{12}\phi_{12} \rightarrow \phi_{12}\phi_{12}) &= 192 \frac{\hat{g}^4}{32} \mu^{2\epsilon} \frac{3}{16\pi^2\epsilon} \\
\Gamma_{1loop}^{\hat{g}^4}(\phi_{12}\phi_{13} \rightarrow \phi_{42}\phi_{43}) &= -64 \frac{\hat{g}^4}{32} \mu^{2\epsilon} \frac{3}{16\pi^2\epsilon}.
\end{aligned}$$

Plugging all of the results above into (3.30) and (3.31) and solving for the K -terms yields

$$\begin{aligned}
K_{a_0} &= \frac{28\hat{a}_0^2 + 3\hat{a}_2^2 + 14\hat{a}_0\hat{a}_2}{8\hat{a}_0\pi^2\epsilon} + \frac{9\hat{g}^4}{64\hat{a}_0\pi^2\epsilon} \\
K_{a_2} &= \frac{7\hat{a}_2^2 + 24\hat{a}_0\hat{a}_2}{8\hat{a}_2\pi^2\epsilon} - \frac{3\hat{g}^4}{16\hat{a}_2\pi^2\epsilon}.
\end{aligned} \tag{3.61}$$

With the expressions for the K -terms as well as for ΔZ_ϕ at hand it is now possible to plug them into the beta function given by eq. (3.20). In order to solve the beta function formula (3.20), it is necessary to restore the original couplings $\hat{a}_i = a_i\mu^{-2\epsilon}$ into the relations (3.61) and (3.59). The beta function can then be recast as

$$\begin{aligned}
\beta_{\hat{a}_i} &= \mu^{-2\epsilon+1} a_i \left(-\frac{\partial K_{a_i}}{\partial \mu} + 2 \frac{\partial \Delta Z_\phi}{\partial \mu} \right) \\
&= \mu^{-2\epsilon+1} a_i \left(-(-2\epsilon\mu^{-1} K_{a_i}) + 2(-2\epsilon\Delta Z_\phi) \right) = \hat{a}_i 2\epsilon K_{a_i} - \hat{a}_i 4\Delta Z_\phi.
\end{aligned} \tag{3.62}$$

Finally, plugging the quantities K_{a_0} , K_{a_2} , and ΔZ_ϕ (with $C_2(\text{Adj.}) = 2$) into the expression for the beta functions above gives full beta functions for the couplings \hat{a}_0 and \hat{a}_2 in the $SO(4)$ Higgs model

$$\begin{aligned}
\beta_{\hat{a}_0} &= \frac{224\hat{a}_0^2 + 24\hat{a}_2^2 + 112\hat{a}_0\hat{a}_2 + 9\hat{g}^4 - 48\hat{a}_0\hat{g}^2}{32\pi^2} \\
\beta_{\hat{a}_2} &= \frac{14\hat{a}_2^2 + 48\hat{a}_0\hat{a}_2 - 3\hat{g}^4 - 12\hat{a}_2\hat{g}^2}{8\pi^2}.
\end{aligned} \tag{3.63}$$

These relations are the final result of this chapter.

4. Running of the couplings a_0 and a_2 in $SO(10)$ - diagrammatic approach

This chapter is devoted to the main goal of this thesis which is the beta functions of the couplings a_0 and a_2 in the Higgs sector of the $SO(10)$ GUT theory. Thanks to the results obtained in the previous section, here the diagrammatic computation will turn out to be more efficient, as the structure of the contributing graphs is now more transparent. Note that all of the results presented in this chapter have been confirmed by a program in Mathematica, which was developed by the author of this thesis.

4.1 $SO(10)$ Higgs model description and the beta functions

The Higgs sector of the $SO(10)$ GUT has been described in Chapter 2. In this Chapter the aim is to evaluate the running of the scalar couplings a_0 and a_2 within the $SO(10)$ model, therefore the relevant part of the Lagrangian (2.10) for the calculations here reads

$$\begin{aligned} \mathcal{L}_\phi = & \frac{1}{4} (F_{\mu\nu})_{ij} (F^{\mu\nu})_{ij} + \frac{1}{4} (D_\mu \phi)_{ij}^\dagger (D^\mu \phi)_{ij} \\ & - \frac{\mu^2}{4} (\phi_{ij} \phi_{ij}) + \frac{a_0}{4} (\phi_{ij} \phi_{ij}) (\phi_{kl} \phi_{kl}) + \frac{a_2}{4} (\phi_{ij} \phi_{ik}) (\phi_{lj} \phi_{lk}). \end{aligned} \quad (4.1)$$

The derivation of beta functions for the couplings a_0 and a_2 within the $SO(10)$ model actually goes the exact same way as it did for the $SO(4)$ model. Hence, the notation and formulae presented in sec.4.2 will be used in this Chapter as well. For the reader's convenience, some of the definitions and results from sec.4.2 are reiterated below.

The wave-function renormalization factor $Z_\phi = 1 + \Delta Z_\phi$ is introduced by $\phi_{ij}^B = \sqrt{Z_\phi} \phi_{ij}$ and the couplings are recast as $\hat{a}_0 = a_0 \mu^{-2\epsilon}$, where μ is a regularization scale.

Within the DR scheme the Lagrangian has the form

$$\begin{aligned} \mathcal{L}_\phi^{DR} = & \frac{1}{4} Z_\phi (D_\mu \phi)_{ij}^\dagger (D^\mu \phi)_{ij} \\ & - \frac{\hat{a}_0 \mu^{2\epsilon}}{4} (\phi\phi)_0 (\phi\phi)_0 - \frac{\hat{a}_2 \mu^{2\epsilon}}{4} (\phi\phi)_2 (\phi\phi)_2 \\ & - \frac{\hat{a}_0 \mu^{2\epsilon} K_{a_0}}{4} (\phi\phi)_0 (\phi\phi)_0 - \frac{\hat{a}_2 \mu^{2\epsilon} K_{a_2}}{4} (\phi\phi)_2 (\phi\phi)_2. \end{aligned} \quad (4.2)$$

The formula for the beta function reads

$$\beta_{\hat{a}_i} = \mu^{-2\epsilon+1} a_i \left(-\frac{\partial K_{a_i}}{\partial \mu} + 2 \frac{\partial \Delta Z_\phi}{\partial \mu} \right). \quad (4.3)$$

To summarize, it is again necessary to evaluate K_{a_0} , K_{a_2} , and ΔZ_ϕ in order to obtain the beta functions of the scalar couplings a_0 and a_2 within the $SO(10)$ Higgs model. The K -terms will be determined in the following sections.

The contribution of the wave-function renormalization factor to the beta function (4.3) was evaluated in sec.4.3 for the $SO(4)$ model. However, the computation goes the same way for the $SO(10)$ model with the only difference being that within $SO(10)$ one now has $C_2(\text{Adj.}) = 8$. Therefore the factor ΔZ_ϕ is given by

$$\Delta Z_\phi = \hat{g}^2 C_2(\text{Adj.}) \frac{3}{16\pi^2 \epsilon} = \hat{g}^2 8 \frac{3}{16\pi^2 \epsilon}. \quad (4.4)$$

4.2 Evaluation of K_{a_0} and K_{a_2}

The contribution of the K -terms to the beta function (4.3) within $SO(10)$ has to be evaluated in a similar manner as it was within $SO(4)$. The counterterms K_{a_0} and K_{a_2} will again be fixed via the equations (where the notation from the previous Chapter is employed)

$$\begin{aligned} \Gamma_{1loop}^1 + \Gamma_{Ka0}^1 + \Gamma_{Ka2}^1 &\stackrel{!}{=} \text{finite} \\ \Gamma_{1loop}^2 + \Gamma_{Ka0}^2 + \Gamma_{Ka2}^2 &\stackrel{!}{=} \text{finite}, \end{aligned} \quad (4.5)$$

where the equality $\stackrel{!}{=} \text{finite}$ means that the counterterms absorb only the pole terms (i.e. the calculation will be done in the MS scheme).

The 4-point functions Γ^1 and Γ^2 are set to be the same as they were in the previous Chapter. This is so because the expectation is that it will be possible to use the knowledge from the calculations within $SO(4)$ to the $SO(10)$ case. Therefore, let the 4-point functions be denoted by

$$\begin{aligned} \Gamma^1 &\equiv \Gamma(\phi_{12}\phi_{12} \rightarrow \phi_{12}\phi_{12}) \\ \Gamma^2 &\equiv \Gamma(\phi_{12}\phi_{13} \rightarrow \phi_{42}\phi_{43}). \end{aligned} \quad (4.6)$$

Since, the index structure of the interaction terms in (4.2) is the same as in (3.15) one can infer that the contributions to the 4-point functions in (4.6) will have the same form, namely

$$\begin{aligned} &\Gamma_{1loop}(\phi_{12}\phi_{12} \rightarrow \phi_{12}\phi_{12}) + \Gamma_{Ka0}(\phi_{12}\phi_{12} \rightarrow \phi_{12}\phi_{12}) \\ &\quad + \Gamma_{Ka2}(\phi_{12}\phi_{12} \rightarrow \phi_{12}\phi_{12}) \stackrel{!}{=} \text{finite} \\ &\Gamma_{1loop}(\phi_{12}\phi_{13} \rightarrow \phi_{42}\phi_{43}) + \Gamma_{Ka0}(\phi_{12}\phi_{13} \rightarrow \phi_{42}\phi_{43}) \\ &\quad + \Gamma_{Ka2}(\phi_{12}\phi_{13} \rightarrow \phi_{42}\phi_{43}) \stackrel{!}{=} \text{finite}. \end{aligned} \quad (4.7)$$

For the 1-loop contributions to the 4-point functions then holds

$$\begin{aligned}
\Gamma_{1loop}(\phi_{12}\phi_{12} \rightarrow \phi_{12}\phi_{12}) &= \Gamma_{1loop}^{\hat{a}_0^2}(\phi_{12}\phi_{12} \rightarrow \phi_{12}\phi_{12}) + \Gamma_{1loop}^{\hat{a}_0\hat{a}_2}(\phi_{12}\phi_{12} \rightarrow \phi_{12}\phi_{12}) \\
&\quad + \Gamma_{1loop}^{\hat{a}_2^2}(\phi_{12}\phi_{12} \rightarrow \phi_{12}\phi_{12}) + \Gamma_{1loop}^{\hat{g}^4}(\phi_{12}\phi_{12} \rightarrow \phi_{12}\phi_{12}) \\
\Gamma_{1loop}(\phi_{12}\phi_{13} \rightarrow \phi_{42}\phi_{43}) &= \Gamma_{1loop}^{\hat{a}_0\hat{a}_2}(\phi_{12}\phi_{13} \rightarrow \phi_{42}\phi_{43}) + \Gamma_{1loop}^{\hat{a}_2^2}(\phi_{12}\phi_{13} \rightarrow \phi_{42}\phi_{43}) \\
&\quad + \Gamma_{1loop}^{\hat{g}^4}(\phi_{12}\phi_{13} \rightarrow \phi_{42}\phi_{43}).
\end{aligned} \tag{4.8}$$

Hence, in order to obtain the K -terms it is necessary to evaluate the contributions to the 4-point functions in (4.7) and (4.8) and this will be done in the following subsections. It is perhaps worth to reiterate that all of the following calculations in this Chapter will be done within the $SO(10)$ model and the MS scheme will be employed (therefore only the pole terms will be computed).

4.2.1 Purely scalar contributions to $\Gamma(\phi_{12}\phi_{12} \rightarrow \phi_{12}\phi_{12})$

There are purely scalar 1-loop contributions to $\Gamma(\phi_{12}\phi_{12} \rightarrow \phi_{12}\phi_{12})$ proportional to \hat{a}_0^2 , \hat{a}_2^2 , and to $\hat{a}_0\hat{a}_2$ (as was also the case in the previous chapter).

First, the contribution $\Gamma_{1loop}^{\hat{a}_0^2}(\phi_{12}\phi_{12} \rightarrow \phi_{12}\phi_{12})$ will be evaluated. In the case of $SO(4)$ the diagrams are depicted in Figure 3.4, from which one can make the following observations. Regarding the combinatorial factors, there are two types of graphs in Figure 3.4 - a diagram with the loop made of ϕ_{12} and the second type contains a 1-loop diagram for every pair of indices (ij) , where $i, j \in \{1, \dots, 10\}$ and $(21) \neq (ij) \neq (12)$. Remarkably, the same structure of diagrams also appears in the $SO(10)$ model, which can be checked by analyzing the index structure in (4.2). Alternatively, this can be verified by the full expansion of the interaction terms in (4.2), which was done via the aforementioned program in Mathematica.

The 1-loop diagrams contributing to $\Gamma_{1loop}^{\hat{a}_0^2}(\phi_{12}\phi_{12} \rightarrow \phi_{12}\phi_{12})$ in the $SO(10)$ model are depicted in Figure 4.1. It is immediately obvious that the structure of the integrals corresponding to the graphs is the same as the one which was derived in the previous chapter. The 1-loop contribution to 4-point function thus reads

$$\Gamma_{1loop}^{\hat{a}_0^2}(\phi_{12}\phi_{12} \rightarrow \phi_{12}\phi_{12}) = P \frac{\hat{a}_0^2}{32} \mu^{2\epsilon} \frac{1}{16\pi^2\epsilon}. \tag{4.9}$$

where P stands for a generic combinatorial factor.

The combinatorial factors emerging from the diagrams in Figure 4.1 will now be evaluated. The first diagram receives a factor with the same structure of contractions as in the case of $SO(4)$ and it also receives the same factors from the interaction terms in (2.10), which means it is equal to $f_d = 4^2 \times \binom{4}{2} \binom{4}{2} 2 \times 4! = 27648$. The rest diagrams on the left-hand side in Figure 4.1 receive a factor (which was derived in Chapter 4) of $f_{\mathcal{L}} \times f_l \times f_o = 8^2 \times \binom{2}{2} \binom{2}{2} 2 \times 4! = 3072$ and there are $n_d = 44$ them (because there are 45 distinct ϕ -fields in total). Altogether, the combinatorial factor is equal to

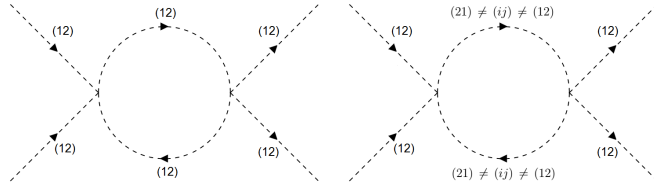


Figure 4.1: 1-loop diagrams contributing to $\Gamma_{1loop}^{\hat{a}_0^2}(\phi_{12}\phi_{12} \rightarrow \phi_{12}\phi_{12})$. As opposed to the $SO(4)$ model there are many more diagrams of the type on the left-hand side in the $SO(10)$ model. This is due to the fact that the indices i, j run through $\{1, \dots, 10\}$.

$$P_1^{a_0^2} = 27648 + 44 \times 3072 = 162816. \quad (4.10)$$

The 1-loop contribution to $\Gamma(\phi_{12}\phi_{12} \rightarrow \phi_{12}\phi_{12})$ proportional to a_0^2 thus reads

$$\Gamma_{1loop}^{\hat{a}_0^2}(\phi_{12}\phi_{12} \rightarrow \phi_{12}\phi_{12}) = 162816 \frac{\hat{a}_0^2}{32} \mu^{2\epsilon} \frac{1}{16\pi^2\epsilon}. \quad (4.11)$$

Next, the 1-loop contributions to $\Gamma(\phi_{12}\phi_{12} \rightarrow \phi_{12}\phi_{12})$ proportional to \hat{a}_2^2 are depicted in Figure 3.8 for the case of the $SO(4)$ model. In order to determine the diagrams for the $SO(10)$ case, one can observe that the condition for the fields ϕ_{ij} creating the loop is that at least one of the indices i and j has to be equal to either 1 or 2. This observation can be verified by expanding the full $SO(10)$ Lagrangian and the diagrams are summarized pictorially in Figure 4.2

As for the combinatorial factors, the first diagram in Figure 4.2 is again one where the loop is made of ϕ_{12} and it receives the same factors from the interaction term as in the $SO(4)$ case. This means that the factor of the first diagram is equal to $f_d = 2^2 \times \binom{4}{2} \binom{4}{2} 2 \times 4! = 6912$. Similarly, the factor responsible for the contractions of one of the diagrams on the right in Figure 4.2 is the same as in the $SO(4)$ model. There are $n_d = 2 \times 8$ viable pairs of indices (again employing the convention of keeping the indices in the ascending order) - because the first index can have both of the values 1 or 2 and the second index then has a choice of 8 remaining indices. Put altogether, the overall combinatorial factor reads

$$P_1^{a_2^2} = 6912 + 16 \times 768 = 19200, \quad (4.12)$$

which means that the 1-loop contribution to $\Gamma(\phi_{12}\phi_{12} \rightarrow \phi_{12}\phi_{12})$ proportional to \hat{a}_2^2 thus reads

$$\Gamma_{1loop}^{\hat{a}_2^2}(\phi_{12}\phi_{12} \rightarrow \phi_{12}\phi_{12}) = 19200 \frac{\hat{a}_2^2}{32} \mu^{2\epsilon} \frac{1}{16\pi^2\epsilon}. \quad (4.13)$$

The last purely scalar 1-loop contribution to $\Gamma(\phi_{12}\phi_{12} \rightarrow \phi_{12}\phi_{12})$ is the one proportional to $\hat{a}_0\hat{a}_2$ and in the $SO(4)$ theory the diagrams are depicted in Figure 3.8. Here one can observe that, pictorially, the diagrams are identical to the ones proportional to \hat{a}_2^2 and the contribution differs only because the factors $f_{\mathcal{L}}$ coming out of the interaction Lagrangian (2.10) for the \hat{a}_2^2 part are not the same as the ones for the $\hat{a}_0\hat{a}_2$ part.

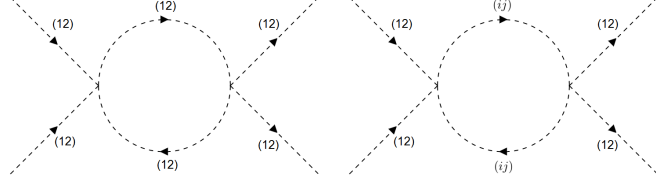


Figure 4.2: 1-loop diagrams contributing to $\Gamma_{1loop}^{\hat{a}_2^2}(\phi_{12}\phi_{12} \rightarrow \phi_{12}\phi_{12})$. In the right diagram at least one of the indices i or j has to be equal to either 1 or 2. The contributions proportional to $\hat{a}_0\hat{a}_2$ have the same structure of Feynman graphs.

Looking again at Figure 4.2, the first diagram receives a factor $f_{\mathcal{L}} = 2 \times 4 \times 2$ from the Lagrangian and the contractions give a factor $f_l \times f_o = \binom{4}{2}\binom{4}{2}2 \times 4!$, hence together the factor is equal to $f_d = 2 \times 4 \times 2 \times \binom{4}{2}\binom{4}{2}2 \times 4! = 27648$. The diagrams on the right in Figure 4.2 receive a factor equal to $f_{\mathcal{L}} = 2 \times 4 \times 8$ from the Lagrangian, the contraction give a factor $f_l \times f_o = \binom{2}{2}\binom{2}{2}2 \times 4!$, and there are $n_d = 2 \times 8$ of such diagrams, which gives an overall factor of $f_d = 2 \times 4 \times 8 \times \binom{2}{2}\binom{2}{2}2 \times 4! \times 2 \times 8 = 49152$. The total factor is then equal to

$$P_1^{\hat{a}_0\hat{a}_2} = 27648 + 49152 = 76800, \quad (4.14)$$

which gives the following 1-loop contribution to $\Gamma(\phi_{12}\phi_{12} \rightarrow \phi_{12}\phi_{12})$ proportional to $\hat{a}_2\hat{a}_0$

$$\Gamma_{1loop}^{\hat{a}_0\hat{a}_2}(\phi_{12}\phi_{12} \rightarrow \phi_{12}\phi_{12}) = 76800 \frac{\hat{a}_0\hat{a}_2}{32} \mu^{2\epsilon} \frac{1}{16\pi^2\epsilon}. \quad (4.15)$$

The contributions of the counterterms $\Gamma_{Ka0}(\phi_{12}\phi_{12} \rightarrow \phi_{12}\phi_{12})$ and $\Gamma_{Ka2}(\phi_{12}\phi_{12} \rightarrow \phi_{12}\phi_{12})$ remains the in the $SO(10)$ model as it was for $SO(4)$ (see (3.45)). This is due to the fact that the diagrams corresponding to the counterterms are tree-level and therefore the extra fields in the $SO(10)$ theory make no difference. For the reader's convenience the contributions of the counterterms to $\Gamma(\phi_{12}\phi_{12} \rightarrow \phi_{12}\phi_{12})$ are reiterated below

$$\begin{aligned} \Gamma_{Ka0}(\phi_{12}\phi_{12} \rightarrow \phi_{12}\phi_{12}) &= -96\mu^{2\epsilon} \frac{\hat{a}_0 K_{\hat{a}_0}}{4} \\ \Gamma_{Ka2}(\phi_{12}\phi_{12} \rightarrow \phi_{12}\phi_{12}) &= -48\mu^{2\epsilon} \frac{\hat{a}_2 K_{\hat{a}_2}}{4}. \end{aligned} \quad (4.16)$$

4.2.2 Purely scalar contributions to $\Gamma(\phi_{12}\phi_{13} \rightarrow \phi_{42}\phi_{43})$

In Chapter 4 there was argued that based on the index structure of the interaction terms that the 4-point function $\Gamma(\phi_{12}\phi_{13} \rightarrow \phi_{42}\phi_{43})$ receives 1-loop contributions only proportional to $\hat{a}_0\hat{a}_2$ and \hat{a}_2^2 (and no 1-loop contributions proportional to \hat{a}_0^2). Since the index structure remains the same when one moves from $SO(4)$ to the $SO(10)$ model, the proposition also holds for the $SO(10)$ case. Therefore, it is necessary to evaluate only the $\hat{a}_0\hat{a}_2$ and \hat{a}_2^2 terms.

To begin with, the 1-loop contribution $\Gamma_{1loop}^{\hat{a}_2^2}(\phi_{12}\phi_{13} \rightarrow \phi_{42}\phi_{43})$ will be evaluated. The relevant diagrams for $SO(4)$ are shown in Figure 3.9. Of course, the

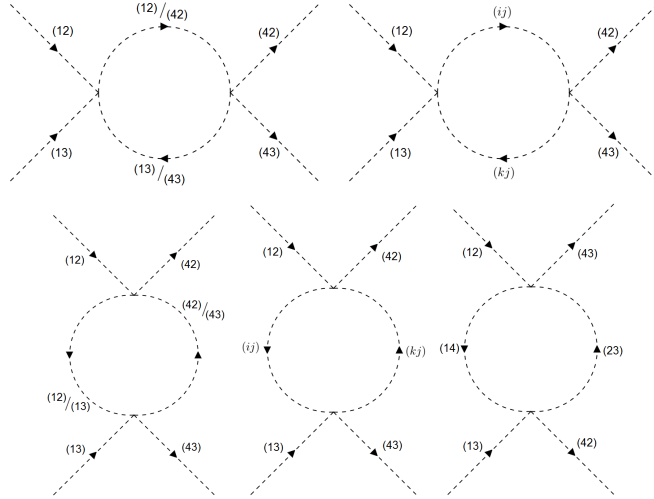


Figure 4.3: 1-loop diagrams contributing to $\Gamma_{1loop}^{a_2^2}(\phi_{12}\phi_{13} \rightarrow \phi_{42}\phi_{43})$. In the first and third diagram the inner lines correspond to either both the ones before the slash or to both the ones after the slash. In the second and fourth diagrams it holds for the inner lines $(ij) \notin \{(12), (13), (42), (43)\}$.

structure of the integrals associated to the diagrams is the same as in the previous subsection but the determination of the combinatorial factors is more elaborate.

A good way to categorize these diagrams (in order to infer the combinatorial factors) consists in looking at which outer legs meet in a vertex. Since there are 4 distinct outer legs, there are $\binom{4}{2} = 6$ unique combinations of 2 outer legs connected to a vertex. However, any given pair of outer legs already determines fully the other pair, therefore there are really only 3 unique categories of diagrams. Furthermore, the combinatorial factors depend on whether the outer legs connecting to a vertex share the same index or not. Last important distinction for determining the factors is whether the loop is made of some of the same fields as the outer legs.

The 1-loop diagrams contributing to $\Gamma_{1loop}^{a_2^2}(\phi_{12}\phi_{13} \rightarrow \phi_{42}\phi_{43})$ are summarized in Figure 4.3. The first and third diagrams in Figure 4.3 receive a factor $f_{\mathcal{L}} = 2 \times 4 \times 8$ from the Lagrangian, the contraction factor is equal to $f_l \times f_o = \binom{2}{1} \binom{2}{1}$, and there are $n_d = 4$ of such diagrams, hence the factor for those diagrams is equal to $f_d = 2 \times 4 \times 8 \times \binom{2}{1} \binom{2}{1} \times 4 = 1024$. The second diagram receives a factor of $f_{\mathcal{L}} = 2 * 8 * 8$ from the Lagrangian and the contraction factor is $f_l \times f_o = 1$. The index structure of the a_2 term in (4.2) dictates that in the second diagram that the inner lines share the index $j \notin \{1, 2, 3, 4\}$ and the other two indices take on the values $i = 2$ and $k = 3$, which means that there are $n_d = 6$ of such diagrams. The total combinatorial factor for the second diagram is thus $f_d = 2 \times 8 \times 8 \times 1 \times 6 = 768$. The fourth diagram has the same structure as the second one when it comes to the combinatorial factor. The fifth diagram receives a factor $f_{\mathcal{L}} = 2 \times 8 \times 8 \times (-1)^3$ and $f_l \times f_o = 1$. Collecting all the factors yields the total combinatorial factor

$$P_2^{a_2^2} = 1024 + 768 + 768 - 128 = 2432, \quad (4.17)$$

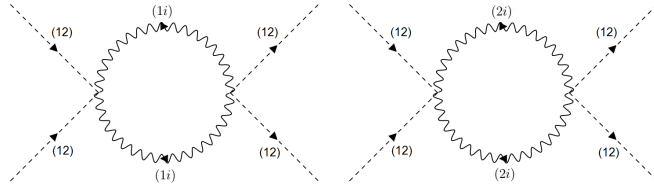


Figure 4.4: 1-loop diagrams contributing to $\Gamma_{1loop}^{\hat{g}_2^4}(\phi_{12}\phi_{12} \rightarrow \phi_{12}\phi_{12})$, where $i \in \{3, \dots, 10\}$.

which means the 1-loop contribution to $\Gamma(\phi_{12}\phi_{13} \rightarrow \phi_{42}\phi_{43})$ proportional to \hat{a}_2^2 reads

$$\Gamma_{1loop}^{\hat{a}_2^2}(\phi_{12}\phi_{13} \rightarrow \phi_{42}\phi_{43}) = 2432 \frac{\hat{a}_2^2}{32} \mu^{2\epsilon} \frac{1}{16\pi^2\epsilon}. \quad (4.18)$$

Another contribution to $\Gamma_{1loop}(\phi_{12}\phi_{13} \rightarrow \phi_{42}\phi_{43})$ is the one proportional to $\hat{a}_0\hat{a}_2$. For $SO(4)$ the diagrams are summarized in Figure 3.10. Remarkably enough, the relevant diagrams in the $SO(10)$ case are exactly the same as they were in $SO(4)$ (including the indices of the fields) and this in turn means the total contribution to the amplitude is

$$\Gamma_{1loop}^{\hat{a}_0\hat{a}_2}(\phi_{12}\phi_{13} \rightarrow \phi_{42}\phi_{43}) = 3072 \frac{\hat{a}_0\hat{a}_2}{32} \mu^{2\epsilon} \frac{1}{16\pi^2\epsilon}. \quad (4.19)$$

Just like in the previous subsection the contribution of the counterterms is the same for the $SO(10)$ model as it was for $SO(4)$ (see (3.50)). Therefore, the contributions of the counterterms to $\Gamma(\phi_{12}\phi_{13} \rightarrow \phi_{42}\phi_{43})$ read

$$\Gamma_{1loop}^{Ka2}(\phi_{12}\phi_{13} \rightarrow \phi_{42}\phi_{43}) = -8\mu^{2\epsilon} \frac{\hat{a}_2 K_{\hat{a}_2}}{4}. \quad (4.20)$$

4.2.3 Contributions to Γ^1 and to Γ^2 proportional to \hat{g}^4

The 1-loop contributions of the gauge fields to $\Gamma(\phi_{12}\phi_{12} \rightarrow \phi_{12}\phi_{12})$ are depicted in Figure 3.11 for $SO(4)$. One can observe from there that the structure of the diagrams is such that the gauge field lines forming the loop are identical and always share exactly 1 index with the outer scalar fields (which implies the other index has to be different from 1 and 2). Indeed, the structure of the indices in the interaction terms in (4.2) dictates that the relevant diagrams in $SO(10)$ are the ones depicted in Figure 4.4.

The structure of the integrals corresponding to the diagrams in Figure 4.4 is the same as it was in the $SO(4)$ case (see (3.53)). Therefore, in $SO(10)$ the contribution from Figure 4.4 has the structure

$$\Gamma_{1loop}^{\hat{g}^4}(\phi_{12}\phi_{12} \rightarrow \phi_{12}\phi_{12}) = P \frac{\hat{g}^4}{32} \mu^{2\epsilon} \frac{3}{16\pi^2\epsilon}. \quad (4.21)$$

As for the combinatorial factors, just like in $SO(4)$ the factors from the Lagrangian together with the contraction factors give $f_d = 2 \times 4! = 48$. The number of contributing graphs is given by the fact that in both of the diagrams in Figure

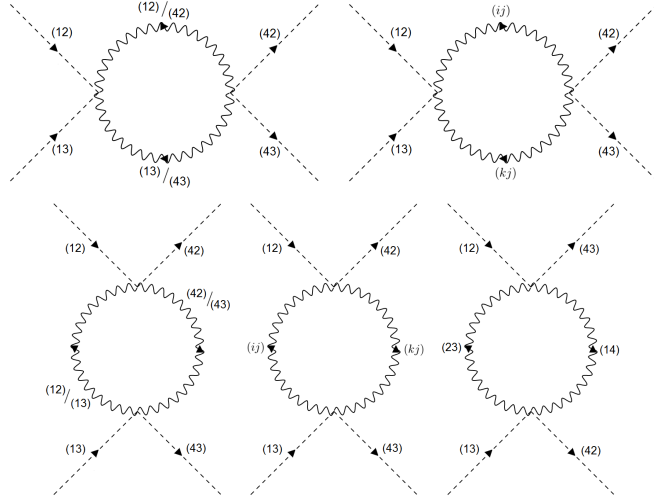


Figure 4.5: 1-loop contributions $\Gamma_{1loop}^{\hat{g}^4}(\phi_{12}\phi_{13} \rightarrow \phi_{42}\phi_{43})$. In the first and third diagram the inner lines are either both the ones before the slash or both the ones after the slash. In the second and fourth diagrams it holds for the inner lines $(ij) \notin \{(12), (13), (42), (43)\}$.

4.4 the index i can have 8 different values; hence $n_d = 16$. The total combinatorial factor is thus equal to

$$P_1^{g^4} = 2 * 4! * 16 = 768. \quad (4.22)$$

This means the 1-loop contribution to $\Gamma(\phi_{12}\phi_{12} \rightarrow \phi_{12}\phi_{12})$ proportional to \hat{g}^4 reads

$$\Gamma_{1loop}^{\hat{g}^4}(\phi_{12}\phi_{12} \rightarrow \phi_{12}\phi_{12}) = 768 \frac{\hat{g}^4}{32} \mu^{2\epsilon} \frac{3}{16\pi^2\epsilon}. \quad (4.23)$$

Lastly, the 1-loop contributions $\Gamma_{1loop}^{\hat{g}^4}(\phi_{12}\phi_{13} \rightarrow \phi_{42}\phi_{43})$ for $SO(4)$ are depicted in Figure 3.12. It useful to compare these 1-loop diagrams to the ones contributing to $\Gamma(\phi_{12}\phi_{13} \rightarrow \phi_{42}\phi_{43})$ which are proportional to \hat{a}_2^2 in Figure 3.9. It is easy to observe that the structure of the diagrams in these two Figures is identical in terms of the index structure and the difference is only that the inner lines are scalars in Figure 3.9 and the inner lines in Figure 3.12 are vectors. In fact, this is also the case in the $SO(10)$ theory, which can be seen by expanding the interaction terms in (4.2). This implies that the 1-loop diagrams contributing to $\Gamma_{1loop}^{\hat{g}^4}(\phi_{12}\phi_{13} \rightarrow \phi_{42}\phi_{43})$ are the ones depicted in Figure 4.5.

The factor f_d for the first and the third diagram in Figure 4.5 receives $f_{\mathcal{L}} = 2 \times (-2) \times 2$ (just like they did in the $SO(4)$ theory) and there are $n_d 4$ such diagrams, which means that the overall factor is $f_d = f_{\mathcal{L}} \times n_d = 2 \times (-2) \times 2 \times 4 = -32$. The second and fourth diagram in Figure 4.5 gets a factor $f_{\mathcal{L}} = 2 \times 2 \times 2$ from the Lagrangian and there are $n_d = 12$ such diagrams, giving an overall factor of $f_d = f_{\mathcal{L}} \times n_d = 2 \times 2 \times 2 \times 12 = 96$. Finally, the fifth diagram gets a factor $f_{\mathcal{L}} = 2 \times (-4) \times 4 = -32$. Collecting all of the factors gives a total combinatorial

factor

$$P_2^{g^4} = -32 + 96 - 32 = 32, \quad (4.24)$$

which means the 1-loop contribution to $\Gamma(\phi_{12}\phi_{13} \rightarrow \phi_{42}\phi_{43})$ proportional to \hat{g}^4 reads

$$\Gamma_{1loop}^{\hat{g}^4}(\phi_{12}\phi_{13} \rightarrow \phi_{42}\phi_{43}) = 32 \frac{\hat{g}^4}{32} \mu^{2\epsilon} \frac{3}{16\pi^2\epsilon}. \quad (4.25)$$

It is necessary to point out that one should also consider diagrams of the type shown in 3.13. There was argued in sec.4.4.3 that these diagrams are finite in the $SO(4)$ model. However, the same arguments hold true also for the $SO(10)$ model and, therefore, the diagrams in Figure 3.13 do not contribute to the beta functions of a_0 and a_2 (or any other beta functions for that matter).

4.3 Beta functions of the couplings a_0 and a_2 in $SO(10)$ Higgs model

The evaluation of the beta functions of a_0 and a_2 in $SO(10)$ follows the same steps as in the $SO(4)$ (see sec. 4.5). Therefore, it is necessary to collect all of the contributions to $\Gamma(\phi_{12}\phi_{12} \rightarrow \phi_{12}\phi_{12})$ and to $\Gamma(\phi_{12}\phi_{13} \rightarrow \phi_{42}\phi_{43})$ from the previous section as well as the wave-function renormalization factor from sec.5.1. The expression for ΔZ_ϕ was given in (4.4) and it reads

$$\Delta Z_\phi = \hat{g}^2 C_2(\text{Adj.}) \frac{3}{16\pi^2\epsilon} = \hat{g}^2 8 \frac{3}{16\pi^2\epsilon} \quad (4.26)$$

where $C_2(\text{Adj.}) = 8$ was used. The K -terms are fixed via the equations (4.7) where one needs to plug in the contributions to $\Gamma(\phi_{12}\phi_{12} \rightarrow \phi_{12}\phi_{12})$ and to $\Gamma(\phi_{12}\phi_{13} \rightarrow \phi_{42}\phi_{43})$ which are given below for the reader's convenience

$$\begin{aligned} \Gamma_{1loop}^{\hat{a}_0^2}(\phi_{12}\phi_{12} \rightarrow \phi_{12}\phi_{12}) &= 162816 \frac{\hat{a}_0^2}{32} \mu^{2\epsilon} \frac{1}{16\pi^2\epsilon} \\ \Gamma_{1loop}^{\hat{a}_2^2}(\phi_{12}\phi_{12} \rightarrow \phi_{12}\phi_{12}) &= 19200 \frac{\hat{a}_2^2}{32} \mu^{2\epsilon} \frac{1}{16\pi^2\epsilon} \\ \Gamma_{1loop}^{\hat{a}_0\hat{a}_2}(\phi_{12}\phi_{12} \rightarrow \phi_{12}\phi_{12}) &= 76800 \frac{\hat{a}_0\hat{a}_2}{32} \mu^{2\epsilon} \frac{1}{16\pi^2\epsilon} \\ \Gamma_{Ka0}(\phi_{12}\phi_{12} \rightarrow \phi_{12}\phi_{12}) &= -96 \mu^{2\epsilon} \frac{\hat{a}_0 K_{\hat{a}_0}}{4} \\ \Gamma_{Ka2}(\phi_{12}\phi_{12} \rightarrow \phi_{12}\phi_{12}) &= -48 \mu^{2\epsilon} \frac{\hat{a}_2 K_{\hat{a}_2}}{4} \\ \Gamma_{1loop}^{\hat{a}_2^2}(\phi_{12}\phi_{13} \rightarrow \phi_{42}\phi_{43}) &= 2432 \frac{\hat{a}_2^2}{32} \mu^{2\epsilon} \frac{1}{16\pi^2\epsilon} \\ \Gamma_{1loop}^{\hat{a}_0\hat{a}_2}(\phi_{12}\phi_{13} \rightarrow \phi_{42}\phi_{43}) &= 3072 \frac{\hat{a}_0\hat{a}_2}{32} \mu^{2\epsilon} \frac{1}{16\pi^2\epsilon} \end{aligned} \quad (4.27)$$

$$\begin{aligned}
\Gamma_{1loop}^{Ka_2}(\phi_{12}\phi_{13} \rightarrow \phi_{42}\phi_{43}) &= -8\mu^{2\epsilon} \frac{\hat{a}_2 K_{\hat{a}_2}}{4} \\
\Gamma_{1loop}^{\hat{g}^4}(\phi_{12}\phi_{12} \rightarrow \phi_{12}\phi_{12}) &= 768 \frac{\hat{g}^4}{32} \mu^{2\epsilon} \frac{3}{16\pi^2\epsilon} \\
\Gamma_{1loop}^{\hat{g}^4}(\phi_{12}\phi_{13} \rightarrow \phi_{42}\phi_{43}) &= 32 \frac{\hat{g}^4}{32} \mu^{2\epsilon} \frac{3}{16\pi^2\epsilon}
\end{aligned}$$

Finally, plugging all of the contributions from (4.27) into the counterterm-fixing equations (4.7) and solving for the K -terms yields

$$\begin{aligned}
K_{\hat{a}_0} &= \frac{106\hat{a}_0^2 + 3\hat{a}_2^2 + 38\hat{a}_0\hat{a}_2}{8\hat{a}_0\pi^2\epsilon} + \frac{9\hat{g}^4}{64\hat{a}_0\pi^2\epsilon} \\
K_{\hat{a}_2} &= \frac{19\hat{a}_2^2 + 24\hat{a}_0\hat{a}_2}{8\hat{a}_2\pi^2\epsilon} + \frac{3\hat{g}^4}{32\hat{a}_2\pi^2\epsilon}.
\end{aligned} \tag{4.28}$$

With the K -terms and the factor ΔZ_ϕ at hand one can plug them into (4.3) (recalling that $\hat{a}_0 = a_0\mu^{-2\epsilon}$) which yields

$$\beta_{\hat{a}_i} = \hat{a}_i 2\epsilon K_{a_i} - \hat{a}_i 4\Delta Z_\phi. \tag{4.29}$$

Finally, plugging the full form of the K -terms from (4.28) and of the factor ΔZ_ϕ from (4.4) into (4.29) gives the full beta functions for the couplings \hat{a}_0 and \hat{a}_2 in **45** in the Higgs sector of the $SO(10)$ GUT

$$\begin{aligned}
\beta_{\hat{a}_0} &= \frac{1}{32\pi^2} \left(848\hat{a}_0^2 + 24\hat{a}_2^2 + 304\hat{a}_0\hat{a}_2 + 9\hat{g}^4 - 192\hat{a}_0\hat{g}^2 \right) \\
\beta_{\hat{a}_2} &= \frac{1}{16\pi^2} \left(76\hat{a}_2^2 + 96\hat{a}_0\hat{a}_2 + 3\hat{g}^4 - 96\hat{a}_2\hat{g}^2 \right).
\end{aligned} \tag{4.30}$$

This is the main result of this thesis. The results in (4.30) have been verified by comparing them with [34].

5. Effective potential method

In this Chapter, the beta functions of the scalar couplings a_0 and a_2 in both the $SO(4)$ Higgs model as well as the $SO(10)$ Higgs model will be evaluated via the Coleman-Weinberg effective potential method introduced in Appendix D. Note that the anomalous dimension part in (D.19) is not easily calculable from the effective potential. Therefore, the term in the beta functions corresponding to the anomalous dimension (which corresponds to the term obtained from the wave-function renormalization factor) will not be evaluated in this chapter. In the final expressions for the beta functions there will be recalled the results for the wave-function renormalization factor from the previous chapters.

5.1 Beta functions of the couplings a_0 and a_2 in the $SO(4)$ Higgs model

First, the relation (D.14) of the scalar coupling a_2 and the $SO(4)$ Higgs potential (3.3) will be identified. Looking at the interaction terms (3.28) and (3.29) (which correspond to the relevant terms in V_ϕ , but with a minus sign, see (3.1)), the coupling a_2 can be expressed as

$$a_2 = \frac{1}{2} \frac{\partial^4 V_\phi(\{\phi_k\})}{\partial \phi_{12} \partial \phi_{13} \partial \phi_{42} \partial \phi_{43}}. \quad (5.1)$$

Since the a_0 -term does not produce any tree-level Feynman diagram which the a_2 term would not contribute to, the a_0 has to be expressed through a more complicated linear combination. Looking again at the interaction terms (3.28) and (3.29), one can infer that the coupling a_0 can be written as

$$a_0 = \frac{1}{24} \frac{\partial^4 V_\phi(\{\phi_k\})}{\partial \phi_{12}^4} - \frac{1}{4} \frac{\partial^4 V_\phi(\{\phi_k\})}{\partial \phi_{12} \partial \phi_{13} \partial \phi_{42} \partial \phi_{43}}. \quad (5.2)$$

The expressions (5.1) and (5.2) can be verified by plugging in for V_ϕ from (3.1). Next, one needs to evaluate are the matrices $W^2(\{\phi_k\})$ and $M^4(\{\phi_k\})$ defined by (D.18), which appear in the right-hand side of (D.19). For this purpose a program in Mathematica was developed.

Having identified the proper derivatives in (5.1) and (5.2) and having evaluated the matrices $W^2(\{\phi_k\})$ and $M^4(\{\phi_k\})$, the Coleman-Weinberg formula (D.19) gives the expressions for the beta functions. Thus, in order to obtain the beta functions for the couplings a_0 and a_2 in the $SO(4)$ Higgs model, it is necessary to plug the derivatives in (5.1) and (5.2) into (D.19) which yields

$$\begin{aligned} \beta_{a_2} &= \frac{1}{32\pi^2} \frac{1}{2} \frac{\partial^4}{\partial \phi_{12} \partial \phi_{13} \partial \phi_{42} \partial \phi_{43}} \left(\text{Tr} [W^2(\{\phi_k\})] + 3 \text{Tr} [M^4(\{\phi_k\})] \right) \\ \beta_{a_0} &= \frac{1}{32\pi^2} \left(\frac{1}{24} \frac{\partial^4}{\partial \phi_{12}^4} - \frac{1}{4} \frac{\partial^4}{\partial \phi_{12} \partial \phi_{13} \partial \phi_{42} \partial \phi_{43}} \right) \times \\ &\quad \left(\text{Tr} [W^2(\{\phi_k\})] + 3 \text{Tr} [M^4(\{\phi_k\})] \right). \end{aligned} \quad (5.3)$$

The derivatives of the matrices W^2 and M^4 in the expressions above read

$$\begin{aligned}
\frac{\partial^4}{\partial\phi_{12}\phi_{13}\phi_{42}\phi_{43}} \text{Tr} [W^2(\{\phi_k\})] &= 16a_2(24a_0 + 7a_2) \\
\frac{\partial^4}{\partial\phi_{12}^4} \text{Tr} [W^2(\{\phi_k\})] &= 96 (56a_0^2 + 52a_0a_2 + 13a_2^2) \\
\frac{\partial^4}{\partial\phi_{12}\phi_{13}\phi_{42}\phi_{43}} \text{Tr} [M^4(\{\phi_k\})] &= -8g^4 \\
\frac{\partial^4}{\partial\phi_{12}^4} \text{Tr} [M^4(\{\phi_k\})] &= 24g^4
\end{aligned} \tag{5.4}$$

Finally, after plugging (5.4) into (5.3) the beta functions of the couplings a_0 and a_2 in the $SO(4)$ Higgs model read

$$\begin{aligned}
\beta_{a_0} &= \frac{224a_0^2 + 24a_2^2 + 112a_0a_2 + 9g^4 - 48a_0g^2}{32\pi^2} \\
\beta_{a_2} &= \frac{14a_2^2 + 48a_0a_2 - 3g^4 - 12a_2g^2}{8\pi^2}.
\end{aligned} \tag{5.5}$$

Note that in the resulting expressions (5.5) the part of the beta function depending on the wave-function renormalization factor (i.e. the part dependent on $a_i g^2$) from Chapter 3 was used (see (3.26) and (3.63)).

The results (5.5) do in fact coincide with the expressions obtained via the diagrammatic approach (see (3.63)). One can observe that the effective potential method has proven to be much more efficient than the diagrammatic approach already for the $SO(4)$ model.

5.2 Beta functions of the couplings a_0 and a_2 in the $SO(10)$ Higgs model

To begin with, it is necessary to express the scalar couplings a_0 and a_2 as fourth derivatives of the Higgs potential V_ϕ in (2.7) (see (D.14)). However, one can observe the index structure of the terms in V_ϕ in (2.7) (which corresponds to the $SO(10)$ model) is the same as the one in (3.28) and (3.29) (which corresponds to the $SO(4)$ model). This in turn means that the couplings a_0 and a_2 in the $SO(10)$ model may be expressed the same way as they were in the $SO(4)$ model, i.e. via the relations (5.1) and (5.2). For the reader's convenience, the relation of the couplings a_0 and a_2 and the potential V_ϕ in the $SO(10)$ model is reiterated below

$$\begin{aligned}
a_0 &= \frac{1}{24} \frac{\partial^4 V_\phi(\{\phi_k\})}{\partial\phi_{12}^4} - \frac{1}{4} \frac{\partial^4 V_0(\{\phi_k\})}{\partial\phi_{12}\phi_{13}\phi_{42}\phi_{43}} \\
a_2 &= \frac{1}{2} \frac{\partial^4 V_\phi(\{\phi_k\})}{\partial\phi_{12}\phi_{13}\phi_{42}\phi_{43}}.
\end{aligned} \tag{5.6}$$

The relations above can be verified by plugging in for V_ϕ from (2.7). After plug-

ging the expressions (5.6) into the Coleman-Weinberg formula (D.19) the beta functions in the $SO(10)$ model have the same form as in (5.3), namely

$$\begin{aligned}\beta_{a_2} &= \frac{1}{32\pi^2} \frac{1}{2} \frac{\partial^4}{\partial \phi_{12} \phi_{13} \phi_{42} \phi_{43}} \left(\text{Tr} \left[W^2(\{\phi_k\}) \right] + 3 \text{Tr} \left[M^4(\{\phi_k\}) \right] \right) \\ \beta_{a_0} &= \frac{1}{32\pi^2} \left(\frac{1}{24} \frac{\partial^4}{\partial \phi_{12}^4} - \frac{1}{4} \frac{\partial^4}{\partial \phi_{12} \phi_{13} \phi_{42} \phi_{43}} \right) \times \\ &\quad \left(\text{Tr} \left[W^2(\{\phi_k\}) \right] + 3 \text{Tr} \left[M^4(\{\phi_k\}) \right] \right).\end{aligned}\tag{5.7}$$

Next, the matrices $W^2(\{\phi_k\})$ and $M^4(\{\phi_k\})$ have to be evaluated within the $SO(10)$ Higgs model. This was done this using an adjusted version of the code in Mathematica, which was mentioned in the previous section. The derivatives of the matrices in (5.7) in the $SO(10)$ model read

$$\begin{aligned}\frac{\partial^4}{\partial \phi_{12} \phi_{13} \phi_{42} \phi_{43}} \text{Tr} \left[W^2(\{\phi_k\}) \right] &= 16a_2(24a_0 + 19a_2) \\ \frac{\partial^4}{\partial \phi_{12}^4} \text{Tr} \left[W^2(\{\phi_k\}) \right] &= 96 \left(212a_0^2 + 100a_0a_2 + 25a_2^2 \right) \\ \frac{\partial^4}{\partial \phi_{12} \phi_{13} \phi_{42} \phi_{43}} \text{Tr} \left[M^4(\{\phi_k\}) \right] &= 4g^4 \\ \frac{\partial^4}{\partial \phi_{12}^4} \text{Tr} \left[M^4(\{\phi_k\}) \right] &= 96g^4\end{aligned}\tag{5.8}$$

Finally, plugging the derivatives of the matrices in (5.8) into (5.7) and adding the term corresponding to the wave-function renormalization factor¹ gives the beta functions of the scalar couplings a_0 and a_2 in the Higgs sector of $SO(10)$ GUT

$$\begin{aligned}\beta_{a_0} &= \frac{1}{32\pi^2} \left(848a_0^2 + 24a_2^2 + 304a_0a_2 + 9g^4 - 192a_0g^2 \right) \\ \beta_{a_2} &= \frac{1}{16\pi^2} \left(76a_2^2 + 96a_0a_2 + 3g^4 - 96a_2g^2 \right).\end{aligned}\tag{5.9}$$

Note that these results in fact coincide with the beta functions obtained through the explicit calculation of the Feynman diagrams (see (4.30)).

The efficiency of the effective potential formalism is displayed in this section in its full glory. While it has taken roughly 10 pages of relatively fast-paced diagrammatic calculations, the effective potential method has arrived at the same result much faster (admittedly, with the help of Mathematica). The results in (5.9) have now been computed in the different ways and they also coincide with the results in [34].

¹This is the part of beta function dependent on $a_i g^2$, see (4.26), (4.30).

Conclusion

In this thesis, the Higgs sector of the minimal $SO(10)$ Grand Unified Theory was studied. It is a well-motivated extension of the Standard Model which, despite its astounding success, is not the complete theory of fundamental particle physics.

GUTs represent a prominent direction within the search for BSM physics because there are multiple hints of a large-energy scale structure including the approximate convergence of the SM gauge couplings as well as the seesaw mechanism.

One of the core aspects which needs to be addressed when constructing a GUT is the Higgs sector. It is responsible for the appropriate symmetry breakdown to the SM gauge group as well as the mass generation within the theory. It has been observed that, at the tree level, the scalar spectrum of the model contains potentially tachyonic pseudo-Goldstone bosons. This would mean that the vacuum structure, chosen so as to produce symmetry breaking chains leading to the SM at low energies, is not necessarily stable. This was the reason why in the 1980s the $SO(10)$ models were dismissed as unphysical.

However, it has been shown recently that quantum effects drastically change the picture. Namely, the 1-loop corrections to the potentially tachyonic masses are able to fix those issues in certain domains of the parameter space.

In order to properly analyze the full picture of the 1-loop approximations, it is necessary to take a look at the running of the scalar couplings (which appear in the formulae for the masses). Furthermore, the coupling a_2 also appears in the tree-level masses of the potentially tachyonic multiplets (see (2.15)).

Another issue connected to the perturbative aspects is the structure of the Landau poles of the couplings in the Higgs sector, as these tend to be close to the unification scale. Having a Landau pole at such energies would bring into question the perturbative approach as a whole and, as such, it is certainly worthwhile to look deeper into the topic.

These questions motivated the endeavor of evaluating the beta functions of at least some scalar couplings within the Higgs sector. This is what was done in this thesis for the couplings a_0 and a_2 appearing in the Higgs potential (2.7). These two couplings play a dominant role when determining the domains of the parameter space of the theory with stable vacua.

The beta functions of the scalar couplings a_0 and a_2 in the Higgs sector of the $SO(10)$ GUT have been computed via two approaches: the explicit evaluation of all the relevant Feynman diagrams (Chapter 4) and the Coleman-Weinberg effective potential method (Chapter 5). Due to the complexity of the diagrammatic approach which is a consequence of having the fairly large 45-dimensional representation of the scalar fields, a simpler $SO(4)$ toy model has been inspected first in Chapter 3. The structure of the interaction terms became much more transparent within the toy model and the results are summarized in (3.63). The expressions for the running couplings have been also verified via the effective potential method in Chapter 5 (see (5.5)).

Thanks to the experience gained in Chapter 3, the calculation of the beta functions of the scalar couplings a_0 and a_2 within the $SO(10)$ theory became much easier as well as better understood. This was very welcome as there is a

big amount of individual relevant diagrams in the larger theory. The explicit evaluation of the Feynman graphs was described in Chapter 4 and the resulting beta functions are given in equation (4.30). This diagrammatic calculation has never been presented before. The beta functions were also computed via the effective potential method (see (5.9)) and the results (4.30) were thus confirmed.

The main results of this thesis (4.30) are important for understanding the perturbative aspects of the minimal $SO(10)$ GUT (as was discussed in more detail in Chapter 2). However, it is appropriate to point out, that in order to fully understand the quantum effects on the masses in the scalar spectrum of the theory, the beta functions of the rest of the scalar couplings contained in the Higgs potential should be evaluated as well. This is in fact a larger ongoing project and this thesis is an effort within that direction.

A. Appendix: $SO(10)$ and its representations

A.1 Basic definitions

Before going into the specifics of $SO(10)$, the reader will be briefly reminded of some basic definitions of Lie group theory and its representations. The introduction into group theory will be rather fast-paced, but it will serve well in terms of fixing the necessary notation.

A *Lie group* G is defined as a differentiable manifold endowed with a smooth group structure (see e.g. [35], [36]).

In this thesis, the following two types of matrix Lie groups are important:

- $SO(N)$ is the special orthogonal group defined as the set of all $N \times N$ matrices M satisfying: $M^T M = M M^T = Id.$ and $\det M = 1.$
- $SU(N)$ is the special unitary group defined as the set of all $N \times N$ matrices U satisfying: $U^\dagger U = U U^\dagger = Id.$ and $\det U = 1.$

The fact that these are matrix groups makes it much easier to work with than it would be with general Lie groups.

The *Lie algebra* \mathfrak{g} associated to a Lie group G is defined as the *tangent space* of G at the identity element. The Lie algebra has a binary operation called the *Lie bracket* which can be defined as a simple commutator when working with matrix groups because one has naturally defined the matrix multiplication. A basis of the Lie algebra is referred to as the set of *generators* X^a which satisfy the commutation relations

$$[X_a, X_b] = i f_{abc} X_c, \quad (\text{A.1})$$

where f_{abc} are the *structure constants*.

In the case of $SO(10)$, the generators of its Lie algebra were defined in (2.2); from there one can infer the commutation relations

$$[\hat{T}^{\alpha\beta}, \hat{T}^{\gamma\delta}] = \frac{i}{\sqrt{2}} \left(\delta^{\alpha\gamma} \hat{T}^{\beta\delta} + \delta^{\beta\delta} \hat{T}^{\alpha\gamma} - \delta^{\beta\gamma} \hat{T}^{\alpha\delta} - \delta^{\alpha\delta} \hat{T}^{\beta\gamma} \right). \quad (\text{A.2})$$

The *representation* of a Lie group is defined as a mapping ρ from the group to the space of automorphisms acting on a representation vector space V . This mapping has to preserve the structure of the group, meaning it is a group homomorphism. Similarly, one can define the representation of a Lie algebra $\tilde{\rho}$ as a mapping from the algebra to the space endomorphisms on a representation vector space and the mapping has to be linear and preserve the algebra's bracket

$$\tilde{\rho}([X, Y]) = \tilde{\rho}(X)\tilde{\rho}(Y) - \tilde{\rho}(Y)\tilde{\rho}(X). \quad (\text{A.3})$$

A special case of a representation is an *irreducible* one which means that the

vector space V has no invariant subspaces (this would be a subspace of V which would be mapped into itself by all of the elements of the algebra).

Relevant examples for this thesis are the irreducible representations of the Lie group $SO(10)$. One important example of an irreducible representation is the *adjoint* representation, defined by the set of matrices

$$[\tilde{T}_a]_{bc} = -if_{abc} \quad (\text{A.4})$$

This is the representation that the Higgs scalar ϕ transforms under.

The *defining* representation of the $SO(10)$ corresponds to ρ being just the identity and thus the representation space is 10-dimensional. This means for a $v \in V$ and $M \in SO(10)$

$$\rho(M)v = Mv. \quad (\text{A.5})$$

From the fundamental representation one can build a general tensor representation, acting on the direct product of the representation spaces of the fundamental representation, i.e. for tensors of the second order one has

$$\rho(M)(v_1 \otimes v_2) = (\rho(M)v_1) \otimes (\rho(M)v_2) = (Mv_1) \otimes (Mv_2). \quad (\text{A.6})$$

In particular, one can build the order 5 tensor representation where the elements in the representation space carry 5 indices v_{ijklm} . However, it turns out that this representation is reducible. In order to construct an order 5 tensor irreducible representation one may take the subspace of tensors with fully antisymmetric indices, i.e. $v_{[ijklm]}$. Using the 10-dimensional Levi-Civita tensor $\epsilon_{ijklmnopqr}$ with the convention $\epsilon_{12345678910} = +1$, one may define the dual map

$$v_{ijklm} \rightarrow \tilde{v} = -\frac{i}{5!} \epsilon_{ijklmnopqr} v_{nopqr}. \quad (\text{A.7})$$

This way it is now possible to define the fully antisymmetric self-dual tensors by

$$\Sigma_{ijklm} := \frac{1}{\sqrt{2}} (v_{ijklm} + \tilde{v}_{ijklm}) \equiv \tilde{\Sigma}_{ijklm} \quad (\text{A.8})$$

This is how the representation of the Higgs scalar Σ -fields in **126** (in Chapter 2) is defined.

A.2 Representations decomposition

In the context of the $SO(10)$ Higgs model studied in this thesis it is useful to take into account the intermediate stages of symmetry breaking, namely $SU(4)_C \otimes SU(2)_L \otimes SU(2)_R$ and $SU(3)_c \otimes SU(2)_L \otimes SU(2)_R \otimes U(1)_{B-L}$. In this section, there will be presented the decomposition of the $SO(10)$ multiplets utilized in this thesis under the subgroups corresponding to the intermediate breaking stage.

Subsequently, it will be shown how they decompose under the SM gauge group. In doing so, results of [37] will be utilized.

The **45** representation of $SO(10)$ decomposes under the $SU(3)_c \otimes SU(2)_L \otimes SU(2)_R \otimes U(1)_{B-L}$ subgroup as

$$45 = (1, 1, 3, 0) \oplus (1, 3, 1, 0) \oplus \left(3, 2, 2, -\frac{2}{3}\right) \oplus \left(\bar{3}, 2, 2, +\frac{2}{3}\right) \\ \oplus (1, 1, 1, 0) \oplus \left(3, 1, 1, +\frac{4}{3}\right) \oplus \left(\bar{3}, 1, 1, -\frac{4}{3}\right) \oplus (8, 1, 1, 0). \quad (\text{A.9})$$

In order to express the decomposition under the SM gauge group, it is useful to recall the relation for the hypercharge

$$Y = T_R^3 + \frac{1}{2}(B - L) \quad (\text{A.10})$$

where T_R^3 corresponds to the third generator of $SU(2)_R$ (analogously to the standard $SU(2)_L$ notation in the SM). For the submultiplets in (A.9) one gets

$$(1, 1, 3, 0) = (1, 1, +1) \oplus (1, 1, 0) \oplus (1, 1, -1), \\ (1, 3, 1, 0) = (1, 3, 0), \\ \left(3, 2, 2, -\frac{2}{3}\right) = \left(3, 2, +\frac{1}{6}\right) \oplus \left(3, 2, -\frac{5}{6}\right), \\ \left(3, 2, 2, +\frac{2}{3}\right) = \left(\bar{3}, 2, -\frac{1}{6}\right) \oplus \left(\bar{3}, 2, +\frac{5}{6}\right), \\ (1, 1, 1, 0) = (1, 1, 0), \\ \left(3, 1, 1, +\frac{4}{3}\right) = \left(3, 1, +\frac{2}{3}\right), \\ \left(\bar{3}, 1, 1, -\frac{4}{3}\right) = \left(\bar{3}, 1, -\frac{2}{3}\right), \\ (8, 1, 1, 0) = (8, 1, 0). \quad (\text{A.11})$$

The fundamental representation of the $SO(10)$ decomposes under the $SU(3)_c \otimes SU(2)_L \otimes SU(2)_R \otimes U(1)_{B-L}$ subgroup as

$$10 = \left(3, 1, 1, -\frac{2}{3}\right) \oplus \left(\bar{3}, 1, 1, +\frac{2}{3}\right) \oplus (1, 2, 2, 0), \quad (\text{A.12})$$

where the submultiplets above decompose under the SM gauge group as

$$\left(3, 1, 1, -\frac{2}{3}\right) = \left(3, 1, -\frac{1}{3}\right), \\ \left(3, 1, 1, +\frac{2}{3}\right) = \left(3, 1, +\frac{1}{3}\right), \\ (1, 2, 2, 0) = \left(1, 2, +\frac{1}{2}\right) \oplus \left(1, 2, -\frac{1}{2}\right). \quad (\text{A.13})$$

The fully antisymmetric self-dual rank 5 tensor representation of the $SO(10)$ decomposes under the $SU(4)_C \otimes SU(2)_L \otimes SU(2)_R$ subgroup as

$$126 = (\bar{10}, 3, 1) \oplus (10, 1, 3) \oplus (6, 1, 1) \oplus (15, 2, 2), \quad (\text{A.14})$$

where the submultiplets above decompose under the SM gauge group as

$$\begin{aligned}
(\overline{10}, 3, 1) &= (6, 3, -\frac{1}{3}) \oplus (3, 3, +\frac{1}{3}) \oplus (1, 3, +1), \\
(10, 1, 3) &= (6, 1, -\frac{1}{3}) \oplus (6, 1, +\frac{2}{3}) \oplus (6, 1, -\frac{4}{3}) \oplus (\overline{3}, 1, +\frac{1}{3}) \\
&\quad \oplus (\overline{3}, 1, -\frac{2}{3}) \oplus (\overline{3}, 1, +\frac{4}{3}) \\
&\quad \oplus (1, 1, 0) \oplus (1, 1, +1) \oplus (1, 1, +2), \\
(15, 2, 2) &= (1, 2, +\frac{1}{2}) \oplus (1, 2, -\frac{1}{2}) \oplus (3, 2, +\frac{1}{6}) \oplus (\overline{3}, 2, -\frac{1}{6}) \\
&\quad \oplus (3, 2, +\frac{7}{6}) \oplus (\overline{3}, 2, -\frac{7}{6}) \oplus (8, 2, +\frac{1}{2}) \oplus (8, 2, -\frac{1}{2}) \\
(6, 1, 1) &= (3, 1, +\frac{1}{3}) \oplus (\overline{3}, 1, -\frac{1}{3}).
\end{aligned} \tag{A.15}$$

Lastly, a single generation of fermions belongs to the 16-dimensional spinorial representation decomposes under the $SU(3)_c \otimes SU(2)_L \otimes SU(2)_R \otimes U(1)_{B-L}$ subgroup as

$$16 = (3, 2, 1, +\frac{1}{3}) \oplus (1, 2, 1, -1) \oplus (3, 1, 2, -\frac{1}{3}) \oplus (1, 1, 2, +1), \tag{A.16}$$

where the submultiplets above decompose under the SM gauge group as

$$\begin{aligned}
(3, 2, 1, +\frac{1}{3}) &= (3, 2, +\frac{1}{6}) \\
(1, 2, 1, -1) &= (1, 2, -\frac{1}{2}) \\
(\overline{3}, 1, 2, -\frac{1}{3}) &= (\overline{3}, 1, +\frac{1}{3}) \oplus (\overline{3}, 1, -\frac{2}{3}), \\
(1, 1, 2, +1) &= (1, 1, +1) \oplus (1, 1, 0)
\end{aligned} \tag{A.17}$$

B. Appendix: Integral methods for the DR procedure

In Chapters 3 and 4 there are described the computations of various 1-loop diagrams which often diverge. In order to tame the divergences the DR procedure is employed. In this Appendix a brief summary of standard formulae used within this procedure is provided. Note that the full treatment of the DR procedure can be found in e.g. [30].

The introduction of Feynman parameters allows one to merge multiple fractional expressions into one fraction. The general formula for two fractions reads

$$\frac{1}{AB} = \int_0^1 dx \frac{1}{[Ax + B(1-x)]^2} \quad (\text{B.1})$$

After the Feynman parameters have been introduced the DR master master can be employed to solve the integral and it reads

$$\int \frac{d^d l}{(2\pi)^d} \frac{(l^2)^r}{(l^2 - C + i\epsilon)^s} = i(-1)^{r-s} \frac{1}{(4\pi)^{d/2}} C^{r-s+\frac{d}{2}} \frac{\Gamma\left(\frac{d}{2} + r\right) \Gamma\left(s - r - \frac{d}{2}\right)}{\Gamma\left(\frac{d}{2}\right) \Gamma(s)}. \quad (\text{B.2})$$

C. Appendix: The interaction term of the $\phi\phi AA$ type

In section 3.4.3 there are the calculations of the contributions to the studied 4-point functions proportional to \hat{g}^4 in the $SO(4)$ model. In order to identify and evaluate the relevant diagrams, it is necessary to inspect the interaction term

$$\begin{aligned}\mathcal{L}_{\phi\phi AA} &= \frac{1}{4}\hat{g}^2\mu^{2\epsilon} [A_\mu, \phi]_{ij}^\dagger [A_\mu, \phi]_{ij} = \\ &= \frac{1}{4}\hat{g}^2\mu^{2\epsilon} \left(A^{ik} A^{il} \phi_{kj} \phi l j + A^{ik} A^{jl} \phi_{kj} \phi_{il} \right).\end{aligned}\tag{C.1}$$

The full expansion of the interaction term reads (lower indices are used for the A-fields for better legibility since the upper index slot is often used by the powers)

$$\begin{aligned}\mathcal{L}_{\phi\phi AA} &= -A_{23}^2\phi_{12}^2 - A_{24}^2\phi_{12}^2 - 2A_{24}A_{34}\phi_{12}\phi_{13} - A_{12}^2\phi_{13}^2 \\ &\quad - A_{23}^2\phi_{13}^2 - A_{34}^2\phi_{13}^2 + 2A_{23}A_{34}\phi_{12}\phi_{14} \\ &\quad - 2A_{23}A_{24}\phi_{13}\phi_{14} - A_{12}^2\phi_{14}^2 - A_{24}^2\phi_{14}^2 \\ &\quad - A_{34}^2\phi_{14}^2 + 2A_{12}A_{2,3}\phi_{12}\phi_{23} - 4A_{12}A_{34}\phi_{14}\phi_{23} \\ &\quad - A_{12}^2\phi_{23}^2 - A_{24}^2\phi_{23}^2 - A_{34}^2\phi_{23}^2 \\ &\quad + 2A_{12}A_{24}\phi_{12}\phi_{24} + 4A_{12}A_{34}\phi_{13}\phi_{24} \\ &\quad + 2A_{23}A_{24}\phi_{23}\phi_{24} - A_{12}^2\phi_{24}^2 - A_{23}^2\phi_{24}^2 \\ &\quad - A_{34}^2\phi_{24}^2 - 2A_{12}A_{24}\phi_{13}\phi_{34} + 2A_{12}A_{23}\phi_{14}\phi_{34} \\ &\quad + 2A_{23}A_{34}\phi_{23}\phi_{34} + 2A_{24}A_{34}\phi_{24}\phi_{34} - A_{23}^2\phi_{34}^2 \\ &\quad - A_{24}^2\phi_{34}^2 - A_{13}^2 \left(\phi_{12}^2 + \phi_{14}^2 + \phi_{23}^2 + \phi_{34}^2 \right) \\ &\quad - A_{14}^2 \left(\phi_{12}^2 + \phi_{13}^2 + \phi_{24}^2 + \phi_{34}^2 \right) \\ &\quad + 2A_{14}(-A_{24}\phi_{13}\phi_{23} + 2A_{23}\phi_{13}\phi_{24} + A_{24}\phi_{14}\phi_{24} \\ &\quad - 2A_{23}\phi_{12}\phi_{34} + A_{34}(\phi_{12}\phi_{23} + \phi_{14}\phi_{34}) \\ &\quad + A_{12}(\phi_{12}\phi_{14} + \phi_{23}\phi_{34})) + 2A_{13}(A_{23}\phi_{13}\phi_{23} \\ &\quad + 2A_{24}\phi_{14}\phi_{23} - A_{34}\phi_{12}\phi_{24} - A_{23}\phi_{14}\phi_{24} \\ &\quad + A_{14}(\phi_{13}\phi_{14} - \phi_{23}\phi_{24}) + 2A_{24}\phi_{12}\phi_{34} \\ &\quad + A_{34}\phi_{13}\phi_{34} + A_{12}(\phi_{12}\phi_{13} - \phi_{24}\phi_{34}))\end{aligned}\tag{C.2}$$

Since the full expression (C.2) is fairly complicated, for the reader's convenience the interaction terms relevant for the calculations in section 4.1.7 are given below. Let the part of the Lagrangian containing the fields $\phi_{ij}\phi_{kl}$ be denoted by $\mathcal{L}_{(ij)(kl)}$. The relevant expressions read

$$\mathcal{L}_{(12)(12)} = \phi_{12}^2 \left(-A_{13}^2 - A_{14}^2 - A_{23}^2 - A_{24}^2 \right),\tag{C.3}$$

$$\mathcal{L}_{(12)(13)} = \phi_{12}\phi_{13}(2A_{12}A_{13} - 2A_{24}A_{34}),\tag{C.4}$$

$$\mathcal{L}_{(12)(24)} = \phi_{12}\phi_{24}(2A_{12}A_{24} - 2A_{13}A_{34}),\tag{C.5}$$

$$\mathcal{L}_{(12)(34)} = \phi_{12}\phi_{34}(-4A_{14}A_{23} + 4A_{13}A_{24}), \quad (\text{C.6})$$

$$\mathcal{L}_{(13)(24)} = \phi_{13}\phi_{24}(4A_{14}A_{23} + 4A_{12}A_{34}), \quad (\text{C.7})$$

$$\mathcal{L}_{(13)(34)} = \phi_{13}\phi_{34}(-2A_{12}A_{24} + 2A_{13}A_{34}), \quad (\text{C.8})$$

$$\mathcal{L}_{(24)(34)} = \phi_{24}\phi_{34}(-2A_{12}A_{13} + 2A_{24}A_{34}). \quad (\text{C.9})$$

D. Appendix: Theory of the effective potential method

The effective potential method was described by J. Goldstone, A. Salam, S. Weinberg in the context of spontaneous symmetry breaking in QFT [28]. S.Coleman and E.Weinberg in their paper 'Radiative Corrections as the Origin of Spontaneous Symmetry Breaking' [29] then further expanded the topic and their work will be presented in this chapter.

In this Appendix, the effective potential will be defined and, subsequently, it will be used it to derive some important results. In Chapter 5, the method will be utilized to evaluating the beta functions of scalar couplings.

The theory of effective potential will be formulated via the path-integral approach, following [29]. Therefore, various basic definitions and results regarding the path-integral formalism will be stated, which can be found in many QFT textbooks, e.g. in [31].

Consider a simple ϕ^4 scalar theory given by the Lagrangian $\mathcal{L}(\phi, \partial_\mu\phi)$ and suppose there is a classical external source $J(x)$ coupled linearly to ϕ

$$\mathcal{L} \rightarrow \mathcal{L} + J(x)\phi(x). \quad (\text{D.1})$$

The standard definition of the *generating functional* reads

$$\begin{aligned} Z[J] &= \int \mathcal{D}\phi \exp \left\{ i \int d^4x [\mathcal{L}(\phi) + J(x)\phi(x)] \right\} \\ &\propto \langle 0, \text{inf} \mid 0, -\infty \rangle_J \end{aligned} \quad (\text{D.2})$$

where the last expression corresponds to the vacuum-to-vacuum transition amplitude in the presence of the external field J . Then, one may define the *connected generating functional* $W[J]$ via the relation

$$e^{iW[J]} := Z[J]. \quad (\text{D.3})$$

Using the quantity W , it is useful define the classical field ϕ_c

$$\phi_c(x) = \frac{\delta W}{\delta J(x)}. \quad (\text{D.4})$$

As the name suggests, the *connected generating functional* W generates connected Green's functions. In other words, W can be expanded in a functional series where the coefficients are the connected Green's functions $G^{(n)}$

$$W = \sum_n \frac{1}{n!} \int d^4x_1 \cdots d^4x_n G^{(n)}(x_1 \cdots x_n) J(x_1) \cdots J(x_n). \quad (\text{D.5})$$

Similarly, one can define a functional called the *effective action* Γ which generates

the contributions of amputated 1PI diagrams $\Gamma^{(n)}$. The effective action is defined as the functional Legendre transformation of W

$$\Gamma(\phi_c) = W(J) - \int d^4x J(x)\phi_c(x), \quad (\text{D.6})$$

which implies

$$J(x) = -\frac{\delta\Gamma}{\delta\phi_c(x)}. \quad (\text{D.7})$$

The effective action can be expanded in a series

$$\Gamma = \sum_n \frac{1}{n!} \int d^4x_1 \cdots d^4x_n \Gamma^{(n)}(x_1 \cdots x_n) \phi_c(x_1) \cdots \phi_c(x_n). \quad (\text{D.8})$$

Crucially, one can also expand the effective action in an alternative manner

$$\Gamma = \int d^4x \left[-V(\phi_c) + \frac{1}{2} (\partial_\mu \phi_c)^2 Z(\phi_c) + \cdots \right]. \quad (\text{D.9})$$

The quantity $V(\phi_c)$ is called the *effective potential* and it will be the central object within the following calculations. One can show, that V can be approximated via the loop expansion, which means it can be expressed as a series, where the coefficients correspond to the sums of all 1PI graphs with k loops, denoted by V_k :

$$V = \sum_{k=0}^{\text{inf}} V_k \left(\frac{\hbar}{2\pi} \right)^k = V_0 + \left(\frac{\hbar}{2\pi} \right) V_1 + O\left(\left(\frac{\hbar}{2\pi} \right)^2 \right). \quad (\text{D.10})$$

Note that, here V_0 is equal to the potential part of the Lagrangian (in other words, it corresponds to the non-derivative terms with a negative sign).

Ultimately, the purpose of introducing the effective potential in the thesis is to calculate the beta functions in the aforementioned Higgs sector. This can be achieved with the help of the renormalization group equation

$$\left(\frac{\partial}{\partial \log \mu} + \beta \frac{\partial}{\partial \lambda} + \gamma_\phi \phi_c \frac{\partial}{\partial \phi_c} \right) V = 0, \quad (\text{D.11})$$

where μ is the *renormalization scale*, λ is the *coupling constant*, β is the *beta function* defined as

$$\beta := \frac{\partial \lambda}{\partial \log \mu} \quad (\text{D.12})$$

and γ is the so-called *anomalous dimension* defined as

$$\gamma_\phi := \frac{1}{2} \frac{1}{Z_\phi} \frac{\partial Z_\phi}{\partial \log \mu}. \quad (\text{D.13})$$

The quantity Z_ϕ is the *wave-function renormalization factor* (also referred to as *field strength renormalization*).

The generalization to a Higgs model with multiple scalar fields $\{\phi_i\}$ and gauge fields $\{A_a\}$ is straightforward. In what follows, the notation introduced in chapter 2 will be used.

Consider a general scalar theory with multiple scalar fields where all the interaction terms are quartic in the scalar fields and suppose there exists a constant C_i such that

$$\lambda_i = C_i \frac{\partial^4 V_0(\{\phi_j\})}{\prod_{i=1}^4 \partial \phi_i}. \quad (\text{D.14})$$

The last expression can be plugged into eq. (D.11), where the appropriate fourth derivative is taken and V is expanded to the 1-loop order

$$\left(\frac{\partial}{\partial \log \mu} + \beta_{\lambda_i} \frac{\partial}{\partial \lambda_i} + \sum_j \gamma_{\phi_j} \frac{\partial}{\partial \phi_j} + \sum_{i=1}^4 \gamma_{\phi_i} \right) C_i \frac{\partial^4 (V_0(\{\phi_i\}) + V_1(\{\phi_i\}, \mu))}{\prod_{i=1}^4 \partial \phi_i} = 0. \quad (\text{D.15})$$

After some manipulations, the equation for the beta function becomes in the leading order

$$\beta_{\lambda_i} = -C_i \frac{\partial^4}{\prod_{j=1}^4 \partial \phi_j} \frac{\partial V_1(\{\phi_i\}, \mu)}{\partial \log \mu} - \sum_{j=1}^4 \gamma_{\phi_j} C_i \frac{\partial^4 V_0(\{\phi_k\})}{\prod_{l=1}^4 \partial \phi_l}. \quad (\text{D.16})$$

Let the first term on the right-hand side of (D.16) be denoted by $\beta_{\lambda_i}^{(1)}$. For the evaluation of $\beta_{\lambda_i}^{(1)}$, one needs to determine the structure of V_1 . This has been done in [29], [10] and after implementing the renormalization conditions (note that the calculations are done in the MS scheme here) it has the form

$$\beta_{\lambda_i}^{(1)} = \frac{1}{32\pi^2} C_i \frac{\partial^4}{\prod_{j=1}^4 \partial \phi_j} \left(\text{Tr} [W^2(\{\phi_k\})] + 3 \text{Tr} [M^4(\{\phi_k\})] \right). \quad (\text{D.17})$$

In the last expression the standard matrix multiplication rule is implicit and the matrices are defined by

$$\begin{aligned} [W(\{\phi_k\})]_{ij} &= \frac{\partial^2 V_0}{\partial \phi_i \partial \phi_j^*} \\ [M^2(\{\phi_k\})]_{ab} &= g^2 \frac{1}{2} \left[(\hat{T}^a \Phi)^\dagger (\hat{T}^b \Phi) + (\hat{T}^b \Phi)^\dagger (\hat{T}^a \Phi) \right] \\ &\equiv g^2 \left[(\hat{T}^a \Phi)^\dagger (\hat{T}^b \Phi) \right]_{(a \leftrightarrow b)} \end{aligned} \quad (\text{D.18})$$

where \hat{T}^a denotes the action of a generator of the Lie algebra associated with the gauge group, Φ denotes the collection of fields $\{\phi_k\}$ in their given representation, and the last equality just corresponds to the symmetrization.

Plugging the expressions (D.17) and (D.14) into (D.16) yields the full beta function

$$\beta_{\lambda_i} = \frac{1}{32\pi^2} C_i \frac{\partial^4}{\prod_{j=1}^4 \partial\phi_j} \left(\text{Tr} [W^2(\{\phi_k\})] + 3 \text{Tr} [M^4(\{\phi_k\})] \right) - \lambda_i \sum_{j=1}^4 \gamma_{\phi_j} \quad (\text{D.19})$$

The last formula is the main result of this Appendix as it provides a straightforward prescription on how to compute the beta function of a gauged quartic scalar theory.

Bibliography

- [1] S. L. GLASHOW, *Partial symmetries of weak interactions*. Nucl. Phys. **22**, pg. 579-588, (1961)
- [2] S. WEINBERG, *A Model of Leptons*. Phys. Rev. vol. **19**, 1264, (1967)
- [3] Y. FUKUDA ET AL., *Evidence for oscillation of atmospheric neutrino*. Phys. Rev. Lett. **81**, pg. 1562-1567 , (1998)
- [4] Q. AHMAD ET AL., *Direct evidence for neutrino flavor transformation from neutral current interactions in the Sudbury Neutrino Observatory*. Phys. Rev. Lett. **89**, 011301, (2002)
- [5] P. PRESS, *Effects of additional scalar decaplet in the RG evolution of the running gauge couplings in the minimal SO(10) grand unified theory*. Available in the Thesis repository of the Charles University: dspace.cuni.cz/handle/20.500.11956/108231 (as of 1.7.2021)
- [6] P. MINKOWSKI, $\mu \rightarrow e\gamma$ at a rate of one out of 109 muon decays?. Phys. Lett. B **67**, pg. 421-428 , (1977)
- [7] H. GEORGI, S. L. GLASHOW, *Unity of All Elementary Particle Forces*. Phys. Rev. Lett. **101**, 438, (1974)
- [8] H. GEORGI, *The state of the art - gauge theories*. AIP Conf. Proc. **23**, pg. 575-828, (1975)
- [9] H. FRITZSCH, P. MINKOWSKI, *Unified Interactions of Leptons and Hadrons*. Annals Phys. **93**, (1975)
- [10] L.GRÁF, M.MALINSKÝ, T.MEDE, V.SUSIČ, *One loop psuedo Goldstone masses in the minimal SO10 Higgs model*. Phys. Rev. D **95**, 075007, (2017)
- [11] L. GRÁF, *Quantum Aspect of Grand Unified Theories*. Available in the Thesis repository of the Charles University: dspace.cuni.cz/handle/20.500.11956/72111 (as of 1.7.2021)
- [12] H. KOLEŠOVÁ, M.MALINSKÝ, *Proton lifetime in the minimal SO(10) GUT and its implications for the LHC*. Phys. Rev. D **90**, 115001, (2014)
- [13] T. DEALTRY, COLL. HYPER-KAMIOKANDE *Hyper-Kamiokande*. Prospects in Neutrino Physics (NuPhys2018) London, 2018, ARXIV:1904.10206
- [14] G. 'T HOOFT, *Magnetic Monopoles in Unified Gauge Theories*. Nucl. Phys. B **79**, pg. 276-284, (1974)
- [15] A. M. POLYAKOV, *Particle Spectrum in the Quantum Field Theory*. JETP Lett. **20**, 194-195, (1974)
- [16] G. G. ROSS, *Grand Unified Theories*. volume v.60 of Frontiers in Physics, The Benjamin/Cummings Publishing Company, Inc., California (1984).

- [17] J. HOŘEJŠÍ, *Fundamentals of Electroweak Theory*. The Karolinum Press, 2002 ISBN 80-246-0639-9
- [18] S.BERTOLINI, L. DI LUZIO, M.MALINSKÝ, *Towards a New Minimal $SO(10)$ Unification*. AIP Conf.Proc. **1467**,pg. 37-44, (2012)
- [19] S.BERTOLINI, L. DI LUZIO, M.MALINSKÝ, *Intermediate mass scales in the nonsupersymmetric $SO(10)$ grand unification: A Reappraisal*. Phys.Rev. D. **80**,015013, (2009)
- [20] S.M.BARR, *A new symmetry breaking pattern for $SO(10)$ and proton decay*. Phys. Lett. B **112**, pg. 219-222 , (1982)
- [21] J.P. DERENDINGER, JIHN E. KIM, DIMITRI V. NANOPOULOS *Anti- $SU(5)$* . Phys. Lett. B vol. **139**, pg. 170-176 , (1984)
- [22] S.BERTOLINI, L. DI LUZIO, M.MALINSKÝ, *Seesaw Scale in the Minimal Renormalizable $SO(10)$ Grand Unification*. Phys. Rev.D **85**, 095014, (2012)
- [23] M. YASUE, *Symmetry Breaking of $SO(10)$ and Constraints on Higgs Potential. 1. Adjoint (45) and Spinorial (16)*. Phys. Rev. D **24**, 1005, (1981)
- [24] M. YASUE, *How to break $SO(10)$ via $SO(4) \times SO(6)$ down to $SU(2)_L \times SU(3)_C \times U(1)$* . Phys. Lett. B **103**, pg. 33-38, (1981)
- [25] G. ANASTAZE, J. P. DERENDINGER, F. BUCCELLA, *Intermediate symmetries in the $SO(10)$ model with $16 \oplus \bar{16} \oplus 45$ Higgses*. Z. Phys. C **20**, pg. 269-273, (1983)
- [26] K. BABU, E. MA, *Symmetry Breaking in $SO(10)$: Higgs Boson Structure*. Phys. Rev. D **31**, pg. 2316-2322, (1985)
- [27] S.BERTOLINI, L. DI LUZIO, M.MALINSKÝ, *On the vacuum of the minimal nonsupersymmetric $SO(10)$ unification*. Phys. Rev.D **81**, 035015, (2010)
- [28] J.GOLDSTONE, A. SALAM, S. WEINBERG, *Broken Symmetries*. Phys. Rev. **127**, pg. 965-970, (1962)
- [29] S.COLEMAN, E.WEINBERG, *Radiative Corrections as the Origin of Spontaneous Symmetry Breaking*. Phys. Rev. D **7**, 1888, (1973)
- [30] M. D. SCHWARTZ, *Quantum Field Theory and the Standard Model*. New York: Cambdrige University Press, 2014. ISBN 1-107-03473-0.
- [31] L.H. RYDER, *Quantum Field Theory*. 2nd edition. Cambridge University Press, 1996. ISBN 0-521-47242-3.
- [32] M. MALINSKÝ, *Higgs Particle Masses in Supersymmetric Models of Electroweak Interactions*.
Available at physics.fjfi.cvut.cz/publications/mf/1996/malinsky_thesis.pdf/
(as of 1.7.2021)
- [33] M. E. PESKIN, D. V. SCHROEDER, *An introduction to quantum field theory*. New York: CRC Press, 2018. ISBN 0-201-50397-5.

- [34] K. JARKOVSKÁ, M. MALINSKÝ, T. MEDE, V. SUSIČ *The minimal potentially realistic $SO(10)$ quantum Higgs model*. In preparation
- [35] M. FECKO, *Differential Geometry and Lie Groups for Physicists*. Cambridge University Press, 2006. ISBN 978-0-511-24521-3.
- [36] H. GEORGI, *Lie Algebras In Particle Physics*. 2nd edition. USA: Westview Press, 1999. ISBN 0-7832-0233-9.
- [37] R.SLANSKY, *Group Theory for Unified Model Building*. Phys .Rept. **79**, (1981)

List of Figures

1.1	Running of the gauge couplings g_s and g in the SM (see [5]).	7
2.1	The sum of QED vacuum polarization loop corrections to all orders.	16
3.1	Feynman rule corresponding to the interaction in (3.22).	22
3.2	The self-energy diagram of a scalar field.	22
3.3	Diagram corresponding to the counterterms K_{a_0} and K_{a_2}	23
3.4	1-loop diagrams contributing to $\Gamma_{1loop}^{\hat{a}_0^2}(\phi_{12}\phi_{12} \rightarrow \phi_{12}\phi_{12})$. The pairs of numbers next to the scalar lines denote the particular scalar fields.	26
3.5	A purely scalar 1-loop diagram.	26
3.6	Feynman rules for the scalar vertex and the scalar propagator.	27
3.7	1-loop diagrams contributing to $\Gamma_{1loop}^{\hat{a}_2^2}(\phi_{12}\phi_{12} \rightarrow \phi_{12}\phi_{12})$	27
3.8	1-loop diagrams contributing to $\Gamma_{1loop}^{\hat{a}_0\hat{a}_2}(\phi_{12}\phi_{12} \rightarrow \phi_{12}\phi_{12})$	28
3.9	1-loop diagrams contributing to $\Gamma_{1loop}^{\hat{a}_2^2}(\phi_{12}\phi_{13} \rightarrow \phi_{42}\phi_{43})$	30
3.10	1-loop diagrams contributing to $\Gamma_{1loop}^{\hat{a}_0\hat{a}_2}(\phi_{12}\phi_{13} \rightarrow \phi_{42}\phi_{43})$	31
3.11	Contributions to $\Gamma_{1loop}^{\hat{g}^4}(\phi_{12}\phi_{12} \rightarrow \phi_{12}\phi_{12})$. For the momenta it holds $p = p_1 + p_2$	32
3.12	Contributions to $\Gamma_{1loop}^{\hat{g}^4}(\phi_{12}\phi_{13} \rightarrow \phi_{42}\phi_{43})$	33
3.13	Diagrams with gauge fields with potentially non-trivial pole terms contributing to $\Gamma(\phi_{12}\phi_{12} \rightarrow \phi_{12}\phi_{12})$ or to $\Gamma(\phi_{12}\phi_{13} \rightarrow \phi_{42}\phi_{43})$	34
4.1	1-loop diagrams contributing to $\Gamma_{1loop}^{\hat{a}_0^2}(\phi_{12}\phi_{12} \rightarrow \phi_{12}\phi_{12})$. As opposed to the $SO(4)$ model there are many more diagrams of the type on the left-hand side in the $SO(10)$ model. This is due to the fact that the indices i, j run through $\{1, \dots, 10\}$	39
4.2	1-loop diagrams contributing to $\Gamma_{1loop}^{\hat{a}_2^2}(\phi_{12}\phi_{12} \rightarrow \phi_{12}\phi_{12})$. In the right diagram at least one of the indices i or j has to be equal to either 1 or 2. The contributions proportional to $\hat{a}_0\hat{a}_2$ have the same structure of Feynman graphs.	40
4.3	1-loop diagrams contributing to $\Gamma_{1loop}^{\hat{a}_2^2}(\phi_{12}\phi_{13} \rightarrow \phi_{42}\phi_{43})$. In the first and third diagram the inner lines correspond to either both the ones before the slash or to both the ones after the slash. In the second and fourth diagrams it holds for the inner lines $(ij) \notin \{(12), (13), (42), (43)\}$	41
4.4	1-loop diagrams contributing to $\Gamma_{1loop}^{\hat{g}^4}(\phi_{12}\phi_{12} \rightarrow \phi_{12}\phi_{12})$, where $i \in \{3, \dots, 10\}$	42
4.5	1-loop contributions $\Gamma_{1loop}^{\hat{g}^4}(\phi_{12}\phi_{13} \rightarrow \phi_{42}\phi_{43})$. In the first and third diagram the inner lines are either both the ones before the slash or both the ones after the slash. In the second and fourth diagrams it holds for the inner lines $(ij) \notin \{(12), (13), (42), (43)\}$	43

List of Tables

1.1	Field content in the SM	6
2.1	Summary of the breaking patterns depending on the structure of the VEVs [10]. There is the so-called 'flipped' $SU(5) \otimes U(1)$ scenario in the last column denoted by $5'1_Z$ described in [20], [21]. .	13

List of Abbreviations

SM	Standard Model
QFT	Quantum field theory
BSM	Beyond Standard Model
GUT	Grand Unified Theory
SO	Special orthogonal group
SU	Special unitary group
VEV	vacuum expectation value
RGE	renormalization group equation
DR	dimensional regularization